CSC Research Reports R02/03

Neuromagnetic source localization using anatomical information and advanced computational methods

Satu Tissari

Finnish IT center for science

Department of Engineering Physics and Mathematics
Helsinki University of Technology
FIN-02150 Espoo, Finland

Neuromagnetic source localization using anatomical information and advanced computational methods

Satu Tissari

Dissertation for the degree of Doctor of Science in Technology
to be presented with due permission of
the Department of Engineering Physics and Mathematics
for public examination and debate
in Auditorium F1 at Helsinki University of Technology (Espoo, Finland)
on the 9th of June, 2003, at 12 noon.

CSC Research Reports R02/03
CSC – Scientific Computing Ltd., Espoo, Finland, 2003

ISSN 0787-7498
ISBN 952-9821-88-3
Picaset Oy, 2003

HELSINKI UNIVERSITY OF TECHNOLOGY P.O. BOX 1000, FIN-02015 HUT http://www.hut.fi	ABSTRACT OF DOCTORAL DISSERTATION

Author Satu Tissari

Name of the dissertation

Neuromagnetic source localization using anatomical information and advanced computational methods

Date of manuscript 6.5.2003	Date of the dissertation 9.6.2003
☐ Monograph	☑ Article dissertation (summary + original articles)

Department	Department of Engineering Physics and Mathematics
Laboratory	Laboratory of Biomedical Engineering
Field of research	Bioelectromagnetism
Opponent(s)	Assistant Professor Thom Oostendorp
Supervisor	Professor Toivo Katila
(Instructor)	Docent Jukka Nenonen

Abstract

Brain function can be studied noninvasively by magnetoencephalography (MEG) which measures weak magnetic fields outside the head. The fields are caused by neural currents, which are often estimated from the measurements. Neuromagnetic source localization results can be combined with individual anatomical information on three-dimensional reconstructions of the subject's brain based on magnetic resonance images. Applying this technique, new significant information was obtained about the continuity of visual perception during eyeblinks in humans. Individual anatomical information can also be used to form realistically shaped volume conductor models in order to improve the neuromagnetic source localization accuracy. It was shown that the whole head MEG with individual brain shaped conductor models can be used to study the cognitive processes associated with deep brain structures like memory functions in the hippocampus.

Advanced computational methods were studied to facilitate the use of realistically shaped conductor models in neuromagnetic source localization. As a first step, the methods were tested with unit spheres and applied to brain shaped homogeneous conductor models using a single current dipole. The accuracy of the forward problem solution, especially near the surface of the conductor model, could be significantly improved using the Galerkin method with linear basis functions. Contrary to a common expectation, the Galerkin method was shown to be efficient and even faster than the widely used collocation method with linear basis functions for a given forward solution accuracy. Large problems could be solved quickly without the explicit formation of the dense matrix with small computer memory requirements using the iterative Bi-CGSTAB method with the precorrected-FFT method.

The methods studied can be applied for MEG, EEG, MCG or ECG with multicompartment volume conductor models and with focused or distributed current source models. The forward problem solution is needed in all bioelectromagnetic source localization. The methods can be taken into routine use for neuromagnetic source localization to improve the source localization accuracy and to decrease the computational costs of accurate modelling.

Keywords Bioelectromagnetism, MEG, image processing, numerical methods

UDC	Number of pages 67+63
ISBN (printed) 952-9821-88-3	ISBN (pdf)
ISBN (others) 951-22-6518-4	ISSN 0787-7498

Publisher CSC-Scientific Computing Ltd.

Print distribution

☑ The dissertation can be read at http://lib.hut.fi/Diss/

to the memory of my father

Preface

This thesis consists of research work performed during three different periods. The first two publications resulted from the work done in 1991-1994 in the Low Temperature Laboratory of Helsinki University of Technology. The third and fourth publication were written in 1998 in CERFACS, Toulouse, France. The last two publications were done in 2000-2002 during my leaves of absence from CSC - Scientific Computing Ltd. I would like to acknowledge the financial support from the Academy of Finland, the Jenny and Antti Wihuri Foundation, the Laboratory of Biomedical Engineering of Helsinki University of Technology, and the Science Foundation of Instrumentarium Corporation.

I would like to thank the late Academician Olli V. Lounasmaa for the possibility to work in the brain research group of the Low Temperature Laboratory. I thank Docent Matti Hämäläinen, my instructor in the Low Temperature Laboratory, and especially my co-authors Academy Professor Riitta Hari and Professor Claudia Tesche for collaboration and their interest in my work.

Professor Ian Duff in CERFACS deserves my full gratitude for providing me excellent working facilities in CERFACS, where I worked as a visiting scientist during my husband's post-doctoral year. Without that this thesis would never have been written.

From the Laboratory of Biomedical Engineering I would like to thank Professor Toivo Katila, my supervisor, for his encouragement and interest in my work. Docent Jukka Nenonen, my instructor and co-author, deserves many thanks for collaboration, his concrete help in numerous situations, comments on manuscripts and continuous encouragement and support.

I would also like to acknowledge the reviewers of my thesis, Dr. Guido Nolte from National Institute of Health in the USA and Docent Pasi Karjalainen from University of Kuopio for their interest and careful reviewing.

At CSC, Managing Director Matti Ihamuotila and Research Director Jari Järvinen flexibly granted me several leaves of absence as was convenient for me. In addition to Matti and Jari I thank my group managers Dr. Mikko Lyly and Docent Janne Ignatius for their support for my research work.

I would like to thank Professor Riitta Salmelin, Mr. Matti Kajola, Pro-

fessor Veijo Virsu and Docent Jari Karhu for good co-authorship and all the people working in the Low Temperature Laboratory, CERFACS, Laboratory of Biomedial Engineering and CSC during my stay for creating a constructive athmosphere. Especially, I would like to give a warm thank to researcher Pirjo-Leena Forsström and Dr. Leila Puska for their friendship.

Finally, I am grateful for my co-author and dear husband Docent Jussi Rahola for a rewarding multidisciplinary collaboration and a deep introduction to his area of expertise, the fascinating world of state-of-the-art numerical methods for integral equations. I thank Jussi for numerous practical advices and constructive comments on the work, his warm support during hard times and his vast patience. Our active spare time made this work possible as it helped both of us to forget the work and relax.

Espoo May 6, 2003

Satu Tissari

Contents

Publications

This thesis consists of this overview and of the following papers.

I R. Hari, R. Salmelin, S. Tissari, M. Kajola, and V. Virsu. Visual stability during eyeblinks. *Nature* **367**, 121–122, 1994.

II C. Tesche, J. Karhu, and S. Tissari. Non-invasive detection of neural population activity in human hippocampus. *Cognitive Brain Research* **4**, 39–47, 1996.

III S. Tissari and J. Rahola. Error analysis of a Galerkin method to solve the forward problem in MEG using the boundary element method. *Computer Methods and Programs in Biomedicine*, 2003. At press. Published earlier as CERFACS Technical Report TR/PA/98/39, CERFACS, 1998.

IV J. Rahola and S. Tissari. Iterative solution of dense linear systems arising from the electrostatic integral equation in MEG. *Physics in Medicine and Biology* **47**, 961–975, 2002.

V S. Tissari and J. Rahola. A precorrected-FFT method to accelerate the solution of the forward problem in MEG. *Physics in Medicine and Biology* **48**, 523–541, 2003.

VI S. Tissari, J. Rahola, and J. Nenonen. Source localization accuracy in MEG using the Galerkin method. In H. Nowak, J. Haueisen, F. Giessler, and R. Huonker, editors, *Proceedings of the 13th International Conference on Biomagnetism, Jena, Germany*, pages 794–797, Berlin, 2002. VDE Verlag.

Author's contributions

In Publication I, the author was responsible for the visualisation of the sources on the 3D MR reconstructions, which was crucial for the interpretation of the results. The tools needed for the segmentation were developed by the author. The author took part in the measurements and commented the manuscript.

In Publication II, a source localization program with realistically shaped conductor models was used to analyze the experimental data. The realistically shaped conductor model was crucial to localize the deep sources. The programs needed to prepare the brain shaped triangular networks were written by the author. The author also studied the use of various realistically shaped conductor models and verified their benefits in source localization accuracy by simulations.

For Publication III, all computer programs to solve the neuromagnetic forward problem using the Galerkin and collocation methods and direct solvers were written by the author. All the test runs for the results were done by the author, who also wrote the paper.

For Publication IV, the iterative methods were added to the programs written by the author for Publication III. The author commented and revised the paper.

For Publication V, the precorrected-FFT method was added to the author's original program. The author got deeply acquainted in the whole code, tested the final code, made some corrections, run the results and wrote the paper.

For Publication VI, the author added the methods for solving the inverse problem to the earlier program. The author planned and run the results and wrote the paper.

Abbreviations

BEM	boundary element method
Bi-CGSTAB	bi-conjugate stabilized algorithm
CSF	cerebral spinal fluid
CT	computed tomography
ECG	electrocardiography
EEG	electroencephalography
FEM	finite element method
FFT	fast Fourier transform
FMM	fast multipole method
fMRI	functional magnetic resonance imaging
GMRES	generalized minimal residual method
ISA	isolated skull approach
MCG	magnetocardiography
MEG	magnetoencephalography
MRI	magnetic resonance imaging
MR	magnetic resonance
NIRS	near infrared spectroscopy
PET	positron emission tomography
PSP	postsynaptic potential
SPECT	single-photon emission computed tomography
SQUID	superconducting quantum interference device
SSP	signal space projection
QMR	quasi-minimal residual method

1 Introduction

Brain function can be studied noninvasively by magnetoencephalography (MEG, [57]) which measures weak magnetic fields outside the head. The fields are caused by the bioelectric activity of neurons. The electric counterpart for MEG is electroencephalography (EEG, [69, 114]) which records the electric potential on the scalp. Other corresponding bioelectromagnetic methods include magneto- and electrocardiography (MCG and ECG, [62]) for heart studies. The temporal resolution of the bioelectromagnetic methods is of the order of a millisecond.

Roughly speaking, the brain consists of the gray matter in the cerebral cortex and the white matter covered by the gray matter. The cortex contains several regions specialized in processing information for example from the various senses of the body, while the white matter contains cabling between various cortical regions. The weak magnetic fields recorded by MEG are the result of simultaneous activity of millions of nearby located neurons mainly in the gray matter.

Other methods for studying the brain function include positron emission tomography (PET, [64]) and single-photon emission computed tomography (SPECT, [68]) which use radioactive tracers to tract metabolic activity of the brain. Near-infrared spectroscopy (NIRS, [130]) detects regional changes in the blood circulation of the brain. This circulation is related to changes in the functional activity of the brain. In addition, functional magnetic resonance imaging (fMRI, [11]) measures changes in the oxygen content of the blood, and thus gives information from the brain activity through cell metabolism. The temporal resolution of all these methods is of the order of few seconds and the spatial resolution from millimeters to centimeters.

In this thesis the localization of bioelectric sources in the brain using MEG is studied. For proper interpretation of MEG recordings the estimated source currents can be combined with the anatomical information of the subject's brain, that can be obtained noninvasively by magnetic resonance imaging (MRI). The source locations can be shown on MR images or more preferably on three-dimensional MR reconstructions. Combining new functional information of the brain with the knowledge of its structure may significantly increase the understanding of the brain function (Publication I).

The neuromagnetic source localization is an inverse problem where

the unknown source which caused the measured magnetic field outside the head is to be found. The neuromagnetic forward problem is to compute the magnetic field outside the head caused by a known source. In practice, the neuromagnetic source localization is based on the repeated solution of the forward problem.

The neuromagnetic inverse problem has no unique solution [131]. However, if the solution is restricted to fulfill some assumptions, a unique solution can be found. A widely used assumption is that the neural activity takes place within a very small region in the brain, and the neural activity can be modelled with a point-like current dipole [134, 25]. In the present thesis this assumption is always used for simplicity. However, the methods to solve the forward problem are independent of the source model.

In addition to the modelling of the neural activity, the volume conductor properties of the head must be described. Traditionally, the human head is modelled with a sphere of isotropic homogeneous conductivity, which, however, is not adequate for all source localization purposes [117, 49]. Especially, the accurate geometrical information available by MRI can be utilized to prepare geometrically more suitable models for the head (Publication II). The conductivity distribution of various head tissues is not available from the anatomical MR images. In principle, some conductivity information may indirectly be obtained via diffusion tensor MR imaging [120]. In the present thesis, the brain conductivity is assumed to be isotropic and homogeneous.

The conductivity assumptions determine which mathematical approach is to be used to solve the inverse problem. In the case of isotropic and homogeneous brain conductivity only the geometry of the conducting regions is included into the conductor model and the boundary element method (BEM) is used. In the case of anisotropic brain conductivity the whole head volume and its surroundings are included into the model and the finite element method (FEM) needs to be used. The mathematical methods used to solve the linear system of equations arising from these two methods are different as the coefficient matrix is dense for the BEM and sparse for the FEM. In addition, the number of elements is typically significantly smaller for the BEM.

The conductivity of the skull is significantly smaller than that of the brain [38]. Thus, the skull isolates the brain from the scalp. For the neuromagnetic source localization it has been shown that it is sufficient to

include only the brain or the inside of the skull to the volume conductor model [59]. In the present thesis, a single-surface realistically shaped conductor model with the BEM is used for the neuromagnetic source localization.

For EEG, the conductor modelling aspects are different. Also the skull and the scalp must be included in the conductor model for EEG source localization, and their conductivities should be known.

In the present thesis, the anatomical information is used to form a realistically shaped conductor model (Publication II) and advanced numerical methods are studied to solve the neuromagnetic forward problem both accurately and efficiently (Publications III–VI).

A motivation to study the brain shaped conductor model is the application of MEG on the functional studies of the deep brain structures like the hippocampus, the thalamus and the brainstem (Publication II). In addition, the frontal-lobe epilepsy is an important application of MEG with the realistically shaped conductor model. Source localization of simultaneous whole head measurements benefits also from a single conductor model instead of several locally fitted spheres for various brain areas [60]. The mathematical methods studied in the present thesis also facilitate new research approaches that depend on accurate forward solutions for realistically shaped geometries. Finally, the neuromagnetic inverse problem has offered a good first application for the studies on the numerical methods because a simple single compartment conductor model can be used to solve the problem. The methods can be examined and developed further for example for EEG source localization, where several layers are needed in the conductor model, and for more complex modelling where the BEM and FEM approaches are combined.

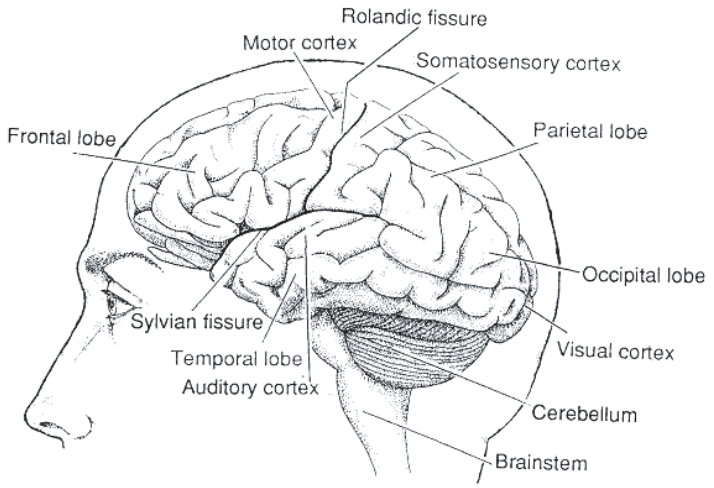

Figure 1: Schematic view of human brain from the left [57]. Presented with the consent of the authors.

2 Magnetoencephalography combined with anatomical images

2.1 Structure and function of the brain

The brain consists of two separate hemispheres which are connected by the corpus callosum. The deep fissure between the hemispheres is called the longitudinal fissure. Both hemispheres consist of frontal, parietal, occipital and temporal lobes (Figure 1). The deep Rolandic fissure separates the frontal and parietal lobes and the deep Sylvian fissure separates the frontal and temporal lobes. The cerebellum is also formed from two hemispheres. Deep brain structures include the brainstem, the cavities full of cerebral-spinal fluid (CSF), together with the hippocampus and the thalamus in each hemisphere. For more details of the brain structure see e.g. [110].

The brain consists of several different cell types with various functions such as the neurons and the glia cells which mainly build the brain. Two main types of neurons, the pyramidal and the stellate cells, form the gray matter which covers the folded surface of the cerebrum, the cerebral cortex. The pyramidal cells tend to be perpendicular to the surface of the cortex (Figure 2). Gray matter is also found in the hippocampus

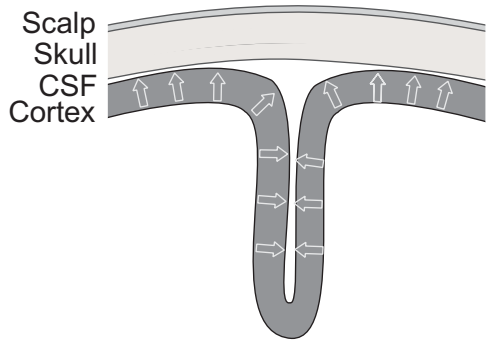

Figure 2: The folded cerebral cortex has a columnar structure such that the pyramidal cells are oriented perpendicularly to the surface of the cortex (arrows). Thus, the neural currents flow mainly as the arrows indicate. MEG is especially sensitive to the current tangential to the brain surface, i.e. the currents in the fissures.

and thalamus. The hippocampus has laminar structures. The inside of the cerebrum consists mostly of the white matter which contains the myelinated axons of the pyramidal neurons. The brain is surrounded by a thin layer of CSF, two brain membranes and finally the skull and the scalp.

Several cortical areas are specialized in processing neural signals from certain senses of the human body. For example, the primary auditory cortex is located in the Sylvian fissure in the temporal lobe, the primary motor cortex in the Rolandic fissure in the frontal lobe, the primary somatosensory cortex in the Rolandic fissure in the parietal lobe and the primary visual cortex in the occipital lobe. These areas respond first to simple sound, somatosensory or visual stimuli and simple movements, correspondingly. There are also special cortical areas for more complex processes such as speech. The areas responding in a complex way to external stimuli are called association cortical areas.

Both the macroscopic and microscopic brain anatomy is complicated. The microscopic anatomy determines the features of the macroscopic source currents to be localized from MEG recordings and the detailed conductivity distribution of the brain tissue. The conductivity of the gray matter is anisotropic, i.e. the pyramidal cells are oriented perpendicularly to the surface of the cortex which makes the current mainly flow in the same direction (Figure 2). The anisotropy is more prominent

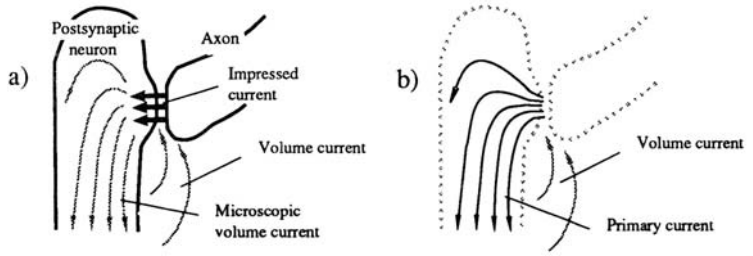

Figure 3: Neural currents generated in a synapse. a) On a microscopic length scale, transmitters released to the synapse between the axon of a neuron and a postsynaptic neuron cause a current through the cell membrane of the postsynaptic neuron called the impressed current and a microscopic volume current inside the neuron. The volume current in the extracellular space encloses the current loop. b) On a macroscopic length scale, the primary current contains the impressed current and part of the microscopic volume currents inside and outside the neuron. Presented with the consent of Risto Ilmoniemi.

in the white matter as the conductivity of the myelinated axon is significantly greater along the axon than along the transverse direction of the axon. The knowledge of the macroscopic anatomy, i.e., the geometry of the brain and the functional specialization of the brain regions are important for the source localization of MEG.

The brain function from the cellular level to the system level is presented in detail in textbooks [114, 69].

2.2 Neural currents

Neurons communicate with each other chemically by releasing transmitters to the synaptic cleft, i.e., the space between axon and dendrite of the two neurons. The transmitters change the permeability of the cell membrane of the postsynaptic cell to certain ions, and thus, cause a change in the membrane potential. This produces an electric field and a current inside the postsynaptic neuron (Figure 3). The postsynaptic potential (PSP) may be either excitatory or inhibitory. The total effect of several simultaneous PSPs may initiate an action potential which travels fast and with undiminished amplitude along the myelinated axon and again causes the transmitter release in the neuron's synapses.

The simultaneous activity of millions of nearby neurons causes an observable magnetic field outside the head [90]. When a small point-like cortical region responses to the given stimulus, the simultaneous postsynaptic potentials drive a current which is called a primary current [99, 62, 119] (Figure 3). The primary current can be approximated with a current dipole, while the currents associated with the traveling action potentials behave more like a current quadrupole. The charge conservation law states that the primary current is compensated by passive ohmic currents, called the volume currents, in the surrounding tissue. Both the primary current and the volume currents generate the magnetic field.

2.3 Measurements

The strength of a typical neuromagnetic signal is 50-500 fT. It is often compared with the earth's magnetic field, which is about 10^9 times stronger. MEG recordings are therefore usually performed in a magnetically shielded room [67], which is necessary to reject outside disturbances such as the fields caused by moving vehicles, radio or power-lines. To be able to measure these weak signals SQUIDs (Superconducting Quantum Interference Device, [140]) are needed. The SQUIDs lay in a dewar filled with liquid helium [3]. In addition, to reduce noise, gradiometers are often used instead of magnetometers. See a recent reference [4] for a more extensive presentation about instrumentation.

Current MEG devices measure the magnetic field (or more precisely certain components of the magnetic field and the gradient of the field) simultaneously in hundreds of locations covering the whole head. A head position indicator system is needed to accurately locate the position of the sensors with respect to the landmarks of the subject's head. The positioning can be done by measuring the magnetic field caused by currents in small coils attached to the scalp and digitizing the locations of the coils with respect to the head's landmarks.

Usually, the spontaneous brain activity or evoked reponses activated by various repeated stimuli or tasks are measured. Evoked responses are averaged to improve the signal-to-noise ratio. Spontaneous brain activity and the heart are sources of noise which cancel out to some extent in the averaging. The off-line data analysis consists typically of digital bandpass filtering and the computation of the field distribution. The noise caused by some external sources may also be reduced by signal

processing methods like signal space projection (SSP) [122]. To interpret the MEG results further, the source of the signals is often searched (magnetic source imaging [62, 6]). In many experimental settings both the spatial and the temporal analyses are important for the interpretation of the data.

Nowadays, extensive experimental work has been done with MEG [89, 86, 51]. MEG has been used to study for example the auditory [46], visual [16], somatosensory [15] and motor systems with evoked responses. MEG has been used in neurology and psychiatry and in cognitive studies. The effect of attention [48], audio-visual interaction [105], responses to faces [73, 44], pain [50], speech processing [104, 91] and human mirror-neuron system [47, 88] are further examples of experimental work. The spontaneous brain activities like cortical oscillations [135, 115] and sleep have been studied by MEG as well as epilepsy [10, 96]. Recordings from deep brain structures such as hippocampus (Publication II) [113], cerebellum [112], thalamus [111, 72] and brainstem [97] have been reported.

The most prominent clinical applications are the localization of epileptic sources as well as the localization of important functional brain regions for presurgical planning [37, 85].

2.4 Imaging of the brain anatomy

Magnetic resonance imaging (MRI, [136]) is the best available imaging method to study the soft tissues of a living human body. In MRI, the subject lies on a bed in a strong homogeneous static magnetic field ranging from 0.23 T to 3 T. In addition, the subject is exposed to short pulses of non-ionising radio-frequency electromagnetic radiation and the signals emitted by the tissues are gathered. Using a certain coding of the radio-frequency transmission, the location of the emitted signal can be obtained by fast Fourier transforms and the slice images can be reconstructed. Depending on the pulse sequence different contrasts between the different tissues can be obtained. MRI is usually safe for the subject, thus it can be easily used for research purposes.

Computerized tomography (CT, [136]), which is based on x-rays, is the best method to image bones as x-rays do not penetrate them easily. X-rays pass the soft tissues almost without attenuating. For example, the structure of the skull can be best obtained by the CT. In contrast, the bony skull does not give any signal in MRI which is based on the

signal obtained from the hydrogen nuclei of water molecules. However, the soft tissues surrounding the skull give a strong signal in MRI, and thus reveal the geometry of the skull.

The imaging accuracy of MRI and CT is of the order of a millimeter. However, in the human body there are several small structures which cannot be accurately imaged. For example, the inner ear structure and the hole in the skull where the auditory nerve penetrates into the brain cannot be seen by either of these imaging methods.

2.5 Visualisation on the 3D MR reconstructions

The anatomical information available in the MR images can be utilized to improve the interpretation of MEG recordings for example by superimposing the estimated sources on the original MR images [56]. The location of the source in a known brain structure allows us to utilize the previous knowledge of the brain function of the source region. Especially, in the case of patients with pathological brain activity it is important to know if there are any structural abnormalities and where the estimated sources are located with respect to them. However, it is not always straightforward to interpret the slice images and, especially, to figure out structures like fissures or gyri which can easily be seen in the three-dimensional reconstructions of the slice images.

To obtain the three-dimensional reconstructions, the brain must be segmented from the MR images, i.e., the contours of the brain are extracted from the surrounding tissues. Digital signal processing provides several segmentation methods such as simple thresholding or region growing from a seed pixel. These procedures can be performed in two or three dimensions. Especially, for a set of MR images containing the same anatomical images with several different tissue contrasts multispectral segmentation and pattern recognition methods can be used. However, no single method works fully automatically and the interactive image processing requires an expert to perform the segmentation. A human visual checking is always needed to ensure the reliability of the results from the medical point of view. Some segmentation methods used in medical imaging are reviewed in [19]. See also [75].

In addition to the segmentation of the brain, a reconstruction method is needed to obtain the final three-dimensional image. However, the difficult task is the segmentation. In practice, if MR images of reasonable quality and segmentation and reconstruction software are available, the

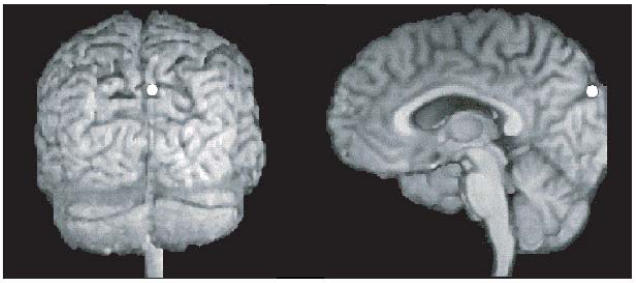

Figure 4: Location (white dot) of brain activation after eyeblinks in three-dimensional MR reconstructions.

three-dimensional reconstructions can be obtained with moderate work.

To be able to superimpose the estimated MEG sources on the MR images or the reconstructions, the two modalities must be registered, i.e. the coordinate systems of the modalities must be aligned. In MEG, the sources are given in the head coordinate system which requires the registration of the head and the MEG device by the head position indicator system [1]. The landmarks of the head coordinate system can be determined in the MR images, and thus, the coordinate transformation can be computed.

In Publication I, the current dipoles were visualized on the three-dimensional MR reconstructions of the subject's brain (Figure 4) and new information could be obtained about the continuity of visual perception during eyeblinks in humans. The sources activated after the eyeblinks were clearly in different locations than conventional early visual evoked responses. The locations of the sources in the subjects' brain structure together with the previous detailed knowledge of the brain function made it possible to create new hypotheses about the spatial working memory system. Similar late responses were reported by EEG six years earlier, but the sources had not been identified [12].

3 Modelling neuromagnetic source localization

3.1 Bioelectromagnetic formulation

For neuromagnetic source localization, the electric field $\vec{E}$ and the magnetic field $\vec{B}$ can be derived from the quasi-static Maxwell equations in linear isotropic media [99]

$$\nabla \times \vec{B} = \mu_0 \vec{J} \quad (1)$$

$$\nabla \times \vec{E} = 0 \quad (2)$$

$$\nabla \cdot \vec{E} = \rho / \epsilon_0 \quad (3)$$

$$\nabla \cdot \vec{B} = 0 \,, \quad (4)$$

where a neural current density $\vec{J}$ is located in the brain having a homogeneous conductivity σ. The permeability of the head is approximately that of the free space, i.e. $\mu = \mu_0$. Here the quasi-static approximation has been used, i.e. $\partial\vec{E}/\partial t = 0$ and $\partial\vec{B}/\partial t = 0$, as in neuromagnetism frequencies below 100 Hz are generally dealt with.

In addition, due to the continuity equation

$$\nabla \cdot \vec{J} = -\frac{\partial \rho}{\partial t} \,, \quad (5)$$

where ρ is the charge density, the neural current density $\vec{J}$ is composed of the driving primary current $\vec{J}^p$ and the passive volume currents $\sigma\vec{E}$ [40, 119, 58]:

$$\vec{J} = \vec{J}^p - \sigma \nabla V \,, \quad (6)$$

where $\vec{E} = -\nabla V$ is applied to obtain the equation for the potential V instead of the electric field $\vec{E}$.

Starting from the Ampère-Laplace law,

$$\vec{B}(\vec{r}) = \frac{\mu_0}{4\pi} \int \frac{\vec{J} \times \vec{R}}{R^3} dv' \,, \quad (7)$$

where $\vec{R} = \vec{r} - \vec{r}'$ and the primed symbols refer to the source region, we can derive the integral formula for the magnetic field

$$\vec{B}(\vec{r}) = \frac{\mu_0}{4\pi} \int (\vec{J}^p + V\nabla'\sigma) \times \frac{\vec{R}}{R^3} dv' \,. \quad (8)$$

From Equation (6) and Equation (1) by taking the divergence of both equations, we obtain the partial differential equation for the potential

$$\nabla \cdot (\sigma \nabla V) = \nabla \cdot \vec{J}^p \,. \quad (9)$$

Using proper boundary conditions the potential can be solved from this equation after which the magnetic field can be solved from Equation (8).

3.2 Piecewise homogeneous conductor model

In practice, it is usually assumed that the conductivity σ_i of various tissues S_i is homogeneous and isotropic. Thus, as $\nabla\sigma$ is nonzero only on the boundaries of the tissues S_{ij}, the integral equation for the magnetic field can be written as the Geselowitz's formula [41]

$$\vec{B}(\vec{r}) = \vec{B}_\infty(\vec{r}) + \frac{\mu_0}{4\pi}\Sigma_{ij}(\sigma_i - \sigma_j)\int_{S_{ij}} V(\vec{r'})\frac{\vec{R}}{R^3}\times d\vec{S'}_{ij}\,, \qquad (10)$$

where

$$\vec{B}_\infty(\vec{r}) = \frac{\mu_0}{4\pi}\int_S \vec{J}^p(\vec{r'})\times\frac{\vec{R}}{R^3}dv' \qquad (11)$$

and S is the infinite medium.

The potential V on the tissue boundaries is needed to compute the magnetic field. Starting from the Green's second identity the following surface integral equation for the potential on the tissue boundaries can be derived [40]:

$$(\sigma_i + \sigma_j)V(\vec{r}) = 2\sigma_0 V_\infty(\vec{r}) - \frac{1}{2\pi}\Sigma_{ij}(\sigma_i - \sigma_j)\int_{S_{ij}} V(\vec{r'})\frac{\vec{R}}{R^3}\cdot d\vec{S}'_{ij}\,, \quad (12)$$

where the potential in an infinite medium is

$$V_\infty = \frac{1}{4\pi\sigma_0}\int_S \vec{J}^p(\vec{r'})\cdot\frac{\vec{R}}{R^3}dv'\,, \qquad (13)$$

and the unit conductivity is $\sigma_0 = 1S/m$.

The above integral equation is well known in potential theory [109] and is related to the exterior Neumann problem for the Laplace equation. The integral equation is a Fredholm equation of the second kind that uses the so-called double-layer representation of the potential. The operator in the equation is called the electrostatic integral operator. On the surface the integral operator becomes singular. The eigenvalues of the above integral equation for a spherical surface are discussed in [2].

3.3 Source models

In neuromagnetic source localization, the neural current sources which cause the measured magnetic field are estimated. The current source

can be modelled, e.g., as a single current dipole [134] or multiple current dipoles [84], when the location, orientation and strength of the dipoles are to be determined. The current source can also be modelled as a set of small current dipoles in fixed locations that are often called distributed currents. In the present thesis, the source is always modelled by a single current dipole.

3.4 Spherically symmetric conductor model

Typically, the head is modelled with a homogeneous sphere, and the neural currents with a current dipole $\vec{J}^p(\vec{r}) = \vec{Q}\delta(\vec{r} - \vec{r}_Q)$, where $\vec{Q}$ is the dipole moment and $\vec{r}_Q$ is the location of the dipole. In that case, the magnetic field outside the head can be computed analytically [106]. There is no need to compute the potential first, thus the computation is very simple and fast.

A further simplification due to the spherical symmetry, is that the volume currents do not contribute to the radial component of the magnetic field but they do contribute to the tangential components of the field [106, 78]. Moreover, any radial conductivity distribution does not affect the field [106].

In addition, for a radial source current the magnetic field vanishes and thus also for any dipolar source in the center of the sphere [106]. Therefore, in a spherically symmetric conductor MEG is sensitive only to the tangential component of the source current. This implies that MEG is optimal for detecting brain activity in the fissures of the cortex.

For the electric potential the spherical symmetry does not bring the above mentioned simplifications. The conductivity distribution as well as the radial current sources and the sources in the center of the sphere affect the potential. In addition, the computation of the potential is more complicated than that of the magnetic field.

With the realistically shaped conductor models the simplifications caused by the spherical model are not valid. Inaccuracies in the shape of the conductor model produce equal distortions in all three components of the magnetic field [59].

3.5 Realistically shaped conductor model

The anatomical information available in MR images can be used to form a realistically shaped conductor model to replace the spherical model

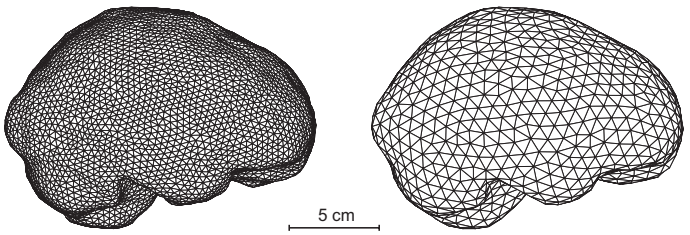

Figure 5: Two examples of a brain shaped boundary element model seen from the subject's right. On the left, there are 10134 triangles, and on the right, 2084 triangles. The segmentation and the triangulation were made by Mika Seppä.

in order to improve the source localization accuracy [54, 63, 59, 79, 117]. In the boundary element method, it is sufficient for MEG that the realistically shaped conductor model encloses the brain or all the tissues inside the skull [59]. This structure isolates the conducting brain tissue from the surrounding conducting tissues. To form the model the brain or the inner surface of the skull needs to be segmented and the brain surface information on each MR slice is combined to form a triangular network (Figure 5). Another approach is to fit an available triangular network to the segmented brain surface information [76].

In addition to the brain, the skull, the scalp and the regions containing the cerebral-spinal fluid can be segmented to be used in more complicated boundary element models or as a part of a hybrid model containing parts modelled with the finite element method.

The conventional anatomical MR images give information about the shapes of various structures in the human body. No information of the tissue conductivities is available in these MR images or by any other imaging modalities. However, attempts have been made to image the anisotropic conductivity of the brain by MRI using pulse sequences that actually image the diffusion of water in the tissues [120]. These MR images can be processed in a similar way than the anatomical MR images and used to form a finite element model of the head. In addition, the segmentation information of the conventional MR images can be combined with the diffusion MR images for the hybrid model.

To obtain a realistically shaped conductor model, the MR images of the subject, the segmentation of the brain and the formation of the triangular network are needed (see Section 2.5). If MR images are not available, a standard model or some other subject's model scaled with

the external size of the head can be used. However, the source localization accuracy will be worse [117, 36]. Thus, the individual models should be the first choice.

In Publication II, brain shaped conductor models, prepared from each subject's individual MR images, were used to study neural sources in or near the hippocampus as well as in the medial temporal lobe. The spherical model is insufficient to model the brain for sources located in these brain structures or regions deep in the brain [117]. In the paper, it was shown that the whole head MEG permits access to cortico-hippocampal neural networks and can be used to evaluate cognitive processes associated to the hippocampal formation such as memory.

3.6 Inverse problem

The neuromagnetic inverse problem is usually solved for a moving single current dipole by a nonlinear least-squares search such as the Levenberg-Marquart algorithm [77] when temporal correlations are ignored. Thus, the forward problem solution, i.e., the potential and the magnetic field due to a current source, is solved several times and the results are compared to the measured data.

The inverse problem can also be solved with the help of lead fields $L_k(\vec{r})$, i.e., the sensitivity distributions of the sensors:

$$b_k = \int_J L_k(\vec{r}) \cdot \vec{J}^p(\vec{r}) dv \ , \tag{14}$$

where b_k is the magnetic field in a sensor k and J is the source region. The corresponding lead fields can be determined also for the electric potential studies. The lead fields are obtained by solving the forward problem for a grid of unit dipoles in the conductor, i.e. a set of unit dipoles in fixed locations. The electric lead fields can be solved using the reciprocal approach [32, 101, 29].

When the source current distribution is estimated using the lead fields an underdetermined linear system is to be solved. The solution, i.e. the moments of the small dipoles, obtained in the sense of L_2 norm is called the minimun-norm estimate [61]. Similarly, when the L_1 norm is used, the minimum-current estimate [124] is obtained. A proper regularization method such as the Tikhonov regularization [116] is often needed [42, 108].

Additional information of the brain can be obtained by other imaging

modalities like anatomic information by MRI and functional information by SPECT, PET or fMRI. This information can be combined with the electromagnetic data to improve the accuracy of the interpretation of the MEG data.

Some attempts have been taken to incorporate anatomical and physiological constraints to restrain the inverse problem formulating it by a probabilistic approach. In a Bayesian approach, probabilistic *a priori* information is used to obtain a solution which best fulfills a certain criterion [5]. Another approach is to obtain a probability distribution for the solution of the inverse problem using Markov chain Monte Carlo (MCMC) methods [13]. See [6] for a recent review on the source estimation.

In all these inverse solution methods, the forward problem needs to be solved either directly for a dipole or as a lead field for a unit dipole in fixed locations. Thus, the accuracy of the forward problem studied in the present thesis affects all source localization studies. Factors affecting the accuracy of the forward problem are described in the next section.

4 Solution of the forward problem

In the present thesis, the brain shaped boundary element conductor model is applied for the neuromagnetic forward problem. As described above, this model has been shown to be sufficient for MEG [59]. The integral equation (12) for the potential on the surface of the model is discretized using the method of weighted residuals from which both the collocation and the Galerkin methods are derived. Constant and linear basis functions are used to model the potential on the boundary elements, i.e. planar triangles. In addition, a method to solve a large problem is presented. The accuracies and the computation times of various methods are compared.

4.1 Method of weighted residuals

In the method of weighted residuals, the unknown function is expanded in terms of basis functions on a computational mesh.

The potential in Equation (12) is expressed as a linear combination of M global basis functions $H_i(\vec{r})$ on the brain shaped triangular network, $(i = 1, ..., M)$:

$$V(\vec{r}) = \sum_{i=1}^{M} V_i H_i(\vec{r}) \; . \tag{15}$$

The coefficients V_i are the unknown values of the potential on the surface of the brain. In the method of weighted residuals both sides of the integral equation are multiplied by a weighting function $W_k(\vec{r})$ and integrated over the surface of S. We obtain the following linear system for the unknown potential values for a single-compartment brain shaped conductor model:

$$\begin{aligned} \sum_{i=1}^{M} V_i \int_S H_i(\vec{r}) W_k(\vec{r}) dS &= 2\frac{\sigma_0}{\sigma} \int_S V^{\infty}(\vec{r}) W_k(\vec{r}) dS \\ -\frac{1}{2\pi} \sum_{i=1}^{M} V_i \int_S \int_S H_i(\vec{r}') \frac{\vec{r} - \vec{r}'}{|\vec{r} - \vec{r}'|^3} \cdot d\vec{S}' W_k(\vec{r}) dS \; , \end{aligned} \tag{16}$$

where $k = 1, \ldots, M$.

The collocation and Galerkin methods can be derived from the above equation using two different kinds of weighting functions [18]. In the collocation method, the weights are delta functions in a set of points called collocation points, while in the Galerkin method the weights are

the basis functions themselves. The Galerkin method tries to satisfy the integral equation everywhere, not only in the collocation points.

Equation (16) holds for an ideal smooth surface on which the whole surface is always seen in a solid angle of 2π [109, 23] (Publication IV). When the surface is described by boundary elements like planar triangles the surface is no more smooth in the vertices of the triangles. In these non-smooth points the whole surface is seen in a solid angle of less than 2π which must be taken into account in the collocation method with linear basis functions as the potential is solved in the vertices of the triangles. This problem is often called an auto-solid angle problem [80]. In the Galerkin method there is no auto-solid angle problem as the potential is solved in a set of points on the triangles.

4.2 Modelling the potential

The basis functions $H_i(\vec{r})$ describe the behaviour of the potential on the surface of the conductor model. In the neuromagnetic boundary element modelling, constant [127, 59, 80, 17], linear [121, 23, 28, 107, 27], quadratic [39, 34] and higher order basis functions [39] have been studied. Eight-noded quadrilateral elements have been used in the electromagnetic cardiographic problem [132, 30, 31]. Usually the collocation method is used, except by Lynn and Timlake [74] who actually used the Galerkin method, though it was not mentioned. Mosher *et al.* [83] and the author (Publication III) studied the Galerkin method independently at the same time. In both works linear basis functions were used.

For the Galerkin method Equation (16) becomes in matrix form

$$(A - B)V = C \,, \tag{17}$$

where the elements of the matrices A and B and the vector C are given by

$$A_{ki} = \int_S H_i(\vec{r}) H_k(\vec{r}) \mathrm{dS} \,, \tag{18}$$

$$B_{ki} = -\frac{1}{2\pi} \int_S \int_S H_i(\vec{r}') \frac{\vec{r} - \vec{r}'}{|\vec{r} - \vec{r}'|^3} \cdot d\vec{S}' H_k(\vec{r}) \mathrm{dS} \,, \tag{19}$$

$$C_i = 2\frac{\sigma_0}{\sigma} \int_S V^\infty(\vec{r}) H_k(\vec{r}) \mathrm{dS} \,. \tag{20}$$

In these equations, A is a sparse matrix and B is a dense matrix.

In Publication III, the accuracy of the collocation method with constant and linear basis functions and the Galerkin method with linear

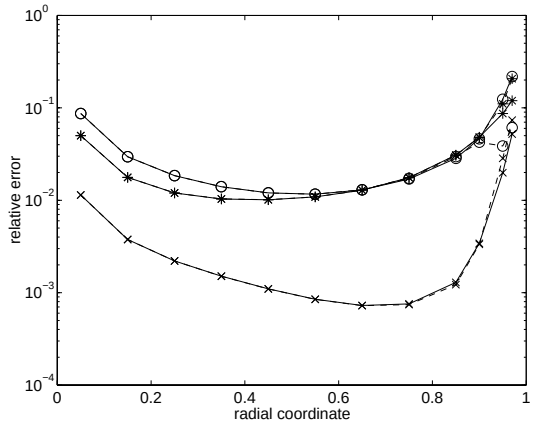

Figure 6: The relative error in the tangential component of the magnetic field as a function of the radial coordinate of the dipole. The number of unknowns is 2252 for the Galerkin and the linear collocation methods and 2000 for the constant collocation method. The lines with o's, *'s, and x's are for the constant and linear collocation methods, and for the Galerkin method, respectively. The solid and dashed lines are for the dipoles under the center of a triangle and under a vertex, respectively.

basis functions was studied for the potential and the magnetic field. The relative error was defined as

$$\text{relative error} = \sqrt{\sum_i (x_i - \hat{x}_i)^2 / \sum_i x_i^2}\,, \tag{21}$$

where x_i refers to the analytic solution and $\hat{x}_i$ refers to the numerical one. The accuracy of the forward solution was studied as a function of the depth of the dipole. The Galerkin method with linear basis functions gave significantly more accurate forward solutions for the tangential component of the magnetic field in the tests with the spherical model (Figure 6). There was essentially no difference between the constant and linear basis functions in the collocation method. The radial component of the magnetic field is not interesting as the volume currents do not contribute to that component of the field in the case of a spherical conductor model. These results agree with those of Mosher *et al.* [83].

In addition, in Publication III the accuracy of the forward solution was studied as a function of the number of unknowns as well as the computation time. The dipole was located at the distance of 0.85 from

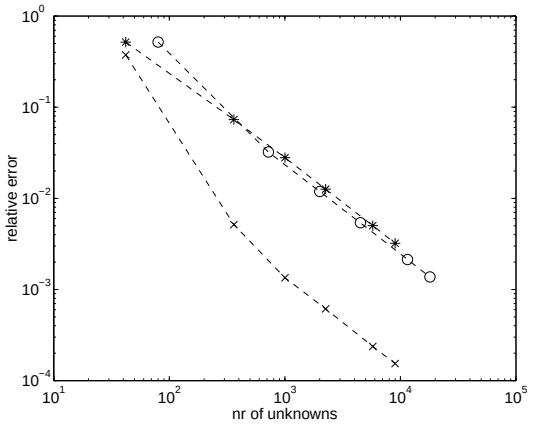

Figure 7: The relative error in the tangential component of the magnetic field as a function of the number of unknowns. The magnetic field is measured around the conductor on a spherical surface of radius $1.3R$. The dashed lines with o's, *'s, and x's are for the constant and linear collocation methods, and the Galerkin method, respectively. Note that both scales are logarithmic.

the origin of the unit sphere. The accuracy improved more steeply with the Galerkin method than with the collocation methods as the number of unknowns increased. The results showed a significant improvement in accuracy with the Galerkin method starting from a few hundreds of unknowns at the realistic measurement distance from the brain (Figure 7). Similarly, the time taken by the matrix construction and the formation of the LU decomposition was significantly smaller for the Galerkin method than for the collocation methods for a given forward problem accuracy. Because a conductor model with less triangles can be used for the Galerkin method to obtain the same accuracy than by the collocation method, the solution time for a new dipole location is shorter for the Galerkin method than for the collocation method (Publication VI).

Finally, in Publication III, the Galerkin method was found to give a much more accurate magnetic field than the collocation methods although the potential was given with roughly similar accuracies by all the methods. In the paper, an explanation for this was given from the point of view of the mathematical error analysis of the boundary element method [109].

4.3 Geometrical elements

In the discretization of the integral equation the simplest boundary elements are planar triangles. With higher order geometrical elements a smooth surface of the conductor model can be obtained. In addition, the real surface of the conducting region may be described more accurately with curved surface elements. In References [39] and [34], isoparametric higher order surface elements have been studied. Bradley *et al.* [14] have analyzed a high-order cubic Hermite boundary element method and compared it to other modelling approaches [59, 107, 80, 83, 39].

In general, the complexity of the computation using various basis functions is determined by the number of unknowns instead of the number of surface elements. Typically, for high-order basis functions the number of unknowns per surface element is higher than for low-order basis functions, e.g., for quadratic basis functions there are usually six unknowns per triangle and for linear basis functions only three.

Comparison of the results of Reference [39] and Publication III shows that the accuracy of the forward problem for the magnetic field may be improved by about the same efficiency using the Galerkin method with simpler basis functions than the collocation method with isoparametric higher order elements with the same number of unknowns.

Frijns *et al.* [34] have shown that the accuracy of the forward problem improved more quickly for quadratic than for linear basis functions as a function of the number of unknowns. The same phenomena was observed for the Galerkin method with linear basis functions (Publication III). Frijns *et al.* [34] have reported that quadratic basis functions for the potential not only improve the accuracy of the forward problem but may also shorten the computation time for the same number of unknowns if compared to linear basis functions. This efficiency is due to the fact that the number of surface elements is reduced by a factor of four.

In the cubic Hermite boundary element method [14] the value and the derivative of the potential are continuous in each node of the mesh. Bradley *et al.* compared results of the collocation based cubic Hermite method to those of the Galerkin method with linear basis functions [83] and reported the cubic Hermite method to be superior to the Galerkin method. It is difficult to compare the absolute error values and the computation times of the Galerkin method (Publication III) and the cubic Hermite method, but the convergence rate, i.e. the improvement in the error as a function of the number of unknowns, can be estimated to be

approximately the same.

The accuracy of the surface discretization with triangles and any other elements can be increased using a large number of elements. This increases the number of unknowns to be solved, and thus, increases the computational costs. However, using curved boundary elements the number of unknowns to be solved per element is greater than that for the triangles. In the present thesis, the accuracy of the surface discretization is increased by increasing the number of triangles instead of using higher order elements.

4.4 Solving a large forward problem

Traditionally, the matrix equation (17) is solved using direct methods such as the LU decomposition [94] or direct inversion obtained by the singular value decomposition [87]. In addition, the approximate inversion of the coefficient matrix with a power series expansion [22] is mentioned in the literature. The computation of the forward solution can be accelerated by calculating the solution directly in the MEG or EEG measurement locations instead of first solving the potential in all nodes of the mesh. For this, a transfer matrix can be precomputed and stored [94, 87, 83]. In the early days the matrix equation was reported to be solved by the Jacobi iteration [7, 74]. Hämäläinen and Sarvas [59] employed the Gauss-Seidel iterative method. The convergence of these iterative methods is slow, they require a lot of memory and need the explicit coefficient matrix like the direct methods.

As the number of unknowns increases the solution of the forward problem will meet two problems. First, the size of the dense matrix increases like N^2, and the computer memory may restrict the number of unknowns to be used. Second, the time to form the dense matrix increases like N^2, the time to compute the LU decomposition like N^3, and the solution with the LU decomposition like N^2. For medium size meshes, the formation of the matrix is the most laborious task, but the time taken by the LU decomposition is also considerable. Unlike these computations, the solution with the LU decomposition is a fast operation.

In the present thesis, advanced numerical methods were studied to replace the LU decomposition in order to solve a large problem efficiently with small computer memory requirements (Publications IV and V). Modern Krylov subspace iterative solvers [8] such as the bi-conjugate

stabilized algorithm (Bi-CGSTAB) [126] (Publication IV) combined with fast methods to compute a matrix-vector multiplication such as the precorrected-FFT method [98] (Publication V) were used to solve large problems quickly without the explicit formation of the dense matrix and the calculation of its LU decomposition. The convergence of the iterative methods was shown to be rapid for both spherical and brain shaped conductor models (Publication IV).

Other modern iterative methods studied were the generalized minimal residual method (GMRES, [103]) and the quasi-minimal residual method (QMR, [33]) (Publication IV). In addition to the precorrected-FFT method, the fast multipole method (FMM) [43] can be used for the fast matrix-vector multiplication. The precorrected-FFT method was chosen because it was estimated to be faster than the FMM.

The precorrected-FFT method is used to compute matrix-vector products quickly in each iteration of the iterative method. In modern iterative methods, the iterates are updated based on the information from successive matrix-vector products $y = Ax$. The vector x is the current iterate of the iterative method and A is the coefficient matrix. The result vector y is used in computing the next iterate. The coefficient matrix is only accessed by these matrix-vector products. Therefore, an approximate solution can be obtained by replacing the exact (explicit) matrix-vector product by an approximate one.

The precorrected-FFT method computes the matrix-vector product approximately and makes the explicit formation of the coefficient matrix unnecessary. Thus, the preprocessing time to form the coefficient matrix and the computer memory requirements are reduced dramatically. The precorrected-FFT method utilizes interpolation operators and the fast Fourier transform (FFT) to rapidly compute the matrix-vector products. For small problems the iterative solution is slower than the solution using the LU decomposition, but for large problems the iteration time is about the same or shorter. The iterative method with the precorrected-FFT method behaves like $N \log N$. The accuracy of precorrected-FFT method is controlled by adjusting method parameters.

In Tables 1 and 2, the computation time and the computer memory needed are presented for the method parameter $p = 3$ by which the accuracy of the method is adjusted. Typical values for p are 2, 3 or 4. For a concrete example, with a triangular mesh of 18 000 triangles the CPU time to solve the forward problem was decreased from 3.5 hours to

Table 1: CPU times (in seconds) for various phases in the computation. The first column gives the number of unknowns. The CPU times are given as follows:
T_{mat}: assembly of the matrix in the direct method,
T_{LU}: computation of the LU decomposition in the direct method,
T_{solve}: solution using the LU decomposition in the direct method,
$T_{\mathrm{p}}(p = 3)$: preprocessing in the precorrected-FFT method,
$T_{\mathrm{it}}(p = 3)$: iterative solution using the precorrected-FFT method.

Unknowns	T_{mat}	T_{LU}	T_{solve}	$T_{\mathrm{p}}(p = 3)$	$T_{\mathrm{it}}(p = 3)$
42	0.2	0.02	0.0005	2.5	0.1
362	15	0.08	0.004	31	0.8
1002	121	1.3	0.09	96	1.5
2252	696	17	0.5	267	3.3
5762	4480	278	1.5	713	11
9002	11600	1110	5.2	1196	27
12962	24100	3560	25	1890	44

Table 2: Memory requirements (in megabytes). Note that the memory sizes include the size of the executable program itself. The first column gives the number of unknowns. The memory requirements are given as follows:
M_{d}: the memory needed in the direct method,
$M_{\mathrm{pFFT}}(p = 3)$: the memory of the precorrected-FFT method.

Unknowns	M_{d}	$M_{\mathrm{pFFT}}(p = 3)$
42	18	18
362	20	22
1002	34	32
2252	98	66
5762	539	126
9002	1288	202
12962	2649	296

less than 5 minutes, and the computer memory requirements from 1.3 GB to 156 MB. Thus, the method makes it possible to use a large number of unknowns to improve the accuracy of the forward problem solution as well as to solve quickly significantly larger problems with widely-used workstations.

As the potential is determined by the integral equation (12) only up to an additive constant, the coefficient matrix $A - B$ in Equation (17) is singular. The singularity is removed by deflation [74]. The correct deflation is essential for the convergence of the iterative methods. The theoretical and numerical eigenvalues of the matrix $A - B$ and the deflation as well as the preconditioning to accelerate the convergence of the iterative method are dealt with in detail in Publication IV.

5 Improved source localization

The motivation for the development of numerical methods for neuromagnetic source localization using realistically shaped boundary element models is to improve the source localization accuracy all over the conductor. The spherical model is generally insufficient for the localization of an arbitrary dipole in the brain. However, there are practical restrictions for the wide use of the realistically shaped conductor models. The need of individual MR images may be overcome by using non-individual conductor models. The advanced numerical methods affect in several ways the source localization procedure, but several other error sources also have an influence on the final source localization accuracy.

5.1 Insufficiency of the spherical model

The widely used spherical conductor model fits to the envelope of the head only locally like in the parietal region. Thus, a single spherical model cannot be found to model the whole head properly. Especially, the frontal lobes are difficult to model by a spherical model. In addition, for simultaneous whole head measurements a single conductor model is more reliable than several locally fitted spheres. A multi-dipole fit for the whole data gives different localization results than independent single dipole fittings for separate subsets of the measurement sensors [60].

The source localization accuracy using the spherical model has been examined both by physical phantom studies and by simulations. The author has investigated the source localization accuracy using a spherical conductor model by simulations [117]. To compute the reference field the collocation method with the constant basis functions was used for a brain shaped conductor model consisting of about 900 triangles. The localization of several dipolar sources of neurophysiological interest in various brain regions was studied. An accuracy of a few millimeters was obtained for superficial dipoles in the brain regions where the spherical model fits well locally to the external head shape. For deep sources and other brain regions the localization errors were up to several centimeters.

First simulation studies of the effect of the head shape on the accuracy of the bioelectromagnetic source localization are presented in Refs. [54, 63, 59, 79, 21]. In References [81] and [118] results similar to the

above mentioned results [59, 117] were concluded. More recently, extensive evaluations of the localization accuracy using thousands of dipoles have been reported [35, 138, 20]. Fuchs *et al.* [35] used a brain shaped conductor model for tangential dipoles. Results similar to earlier evaluations were obtained, except that the maximum localization error was about 45 mm.

Crouzeix *et al.* [20] evaluated the source localization accuracy for MEG by comparing the spherical model, a brain shaped conductor model and a three-layer realistically shaped model. The collocation method with linear basis functions and the isolated skull approach [59] were applied to compute the forward problem solution. The reference field was calculated using 1 500 nodes per layer for the three-layer realistically shaped model. The conclusions presented earlier were confirmed, i.e., the spherical model gives significantly larger localization errors for deep dipoles than for superficial ones. Especially, significantly larger localization errors were obtained for dipoles located in the lower parts of the brain such as the temporal lobe. Merlet *et al.* [82] report similar results using spherical models for the localization of the epileptic sources. In addition, Crouzeix *et al.* [20] reported that the accuracy using a three-layer realistically shaped model was about 2 millimeters better than using a brain shaped conductor model. The number of nodes was the same in both models.

First phantom studies to estimate the MEG source localization errors were reported in Refs. [9, 133, 81]. More recently Leahy *et al.* [71] recorded experimental bioelectromagnetic data for several dipoles in a realistic skull phantom. They performed computer simulations to study the effect of the uncertainty of the tissue conductivities, the simplifications of the spherical conductor model and the numerical errors of the realistically shaped conductor model on the source localization accuracy. The forward solutions were computed using the collocation method with linear basis functions. For MEG, locally fitted single compartment spherical models were used for the somatosensory and the visual brain areas. They concluded that the locally fitted spherical model gives almost as good localization accuracy as the realistically shaped conductor model for MEG. Their localization accuracy was about 3 mm and the registration error about 2 mm.

As a critisism for their study, mainly superficial dipoles in the somatosensory and in the visual cortex were included. For these brain

regions the locally fitted spherical model is sufficient, but similar conclusions cannot be made for regions of more complicated geometry like frontal or temporal lobes. Two frontal dipoles were reported to give the poorest results. Thus, the conclusion is valid only for the superficial dipoles in the brain areas of locally spherical shape. In addition, for the localization of superficial dipoles the Galerkin method with linear basis functions gives more accurate results than the collocation method used in their study (Publication IV).

In general, the tendency has been that when more accurate and more sophisticated phantom studies and simulations have been performed, a wider range of localization error estimates has been obtained. The basic observation has remained unchanged: for superficial dipoles in brain areas of locally spherical shape the localization errors are smaller than for deep dipoles and dipoles in brain areas of non-spherical shape.

5.2 Non-individual realistically shaped conductor models

MR images and segmentation and triangulation software are needed for the individual brain shaped conductor models. Standard models and meshes scaled according to subject's external head shape have been studied to replace the individual realistically shaped conductor models [117, 128, 45, 36].

To avoid the need of the individual MR images the author has studied the scaling of a standard brain shaped network according to the external shape of the head [117]. In addition, the author has studied the scaling of another subject's brain shaped network with the help of the subject's individual MR images to fit the subject's brain [117]. Such scaled models make it possible to avoid the segmentation and the triangulation. The localization accuracy of the individual brain shaped conductor model was significantly better compared to the scaled networks. The network scaled with the external shape of the head gave the worst results though better than the spherical model. Thus, for accurate source localization the individual conductor model is needed.

Van't Ent *et al.* [128] described a set of precisely segmented brain, skull and scalp surfaces from MR images by an expansion in spherical harmonics which was then used to obtain approximate segmentations for other subjects by adjusting the parameters of the spherical harmonics expansion. The adjustment of the parameters was performed using the subject's MR images or the 3D digitization of the subject's scalp. The

brain shaped conductor models were used in MEG source localization. The most accurate results were obtained using an expansion in spherical harmonics adjusted by the subject's MR images. When the MR images were not available good localization results could be obtained using the model adjusted by the digitization of the subject's scalp. The spherical model yielded biggest localization errors.

Haque *et al.* [45] proposed an alternative method to obtain a realistically shaped conductor model without individual MR images. The radial distances of corresponding points on the brain, scalp and skull were collected, and the mean ratios of the radial distances of the brain and the scalp and of the skull and the scalp were obtained. Based on these mean ratios, the brain and skull surfaces of a new subject were estimated from the digitization of the scalp. The estimated volume conductor models were about as accurate as those reported in [128].

Fuchs *et al.* have used averaged MR image data sets for segmentation and mesh generation in order to create standard realistically shaped conductor models [36]. The standard models make it possible to avoid the need of individual MR images and to perform precomputations only once and store them. However, the source localization accuracy is not as good as with individual models but significant improvement can be obtained if compared to the results obtained using the spherical model.

5.3 Effect of advanced mathematical methods

In the present thesis the improvement of the source localization accuracy using the Galerkin method was studied. Linear basis functions and a large number of unknowns were used for comparing the results to the commonly used collocation method with linear basis functions (Publication VI). In addition, the number of unknowns needed for accurate source localization was studied.

To study improvements in the source localization accuracy, a precise brain shaped conductor model of thousands of triangles is needed for a proper reference magnetic field. For this purpose the iterative biconjugate gradient stabilized (Bi-CGSTAB) algorithm with the precorrected-FFT method was necessary.

Simulations showed that the Galerkin method improves significantly the source localization accuracy, compared to the collocation method, both deep in the brain and close to the brain surface. Especially, very

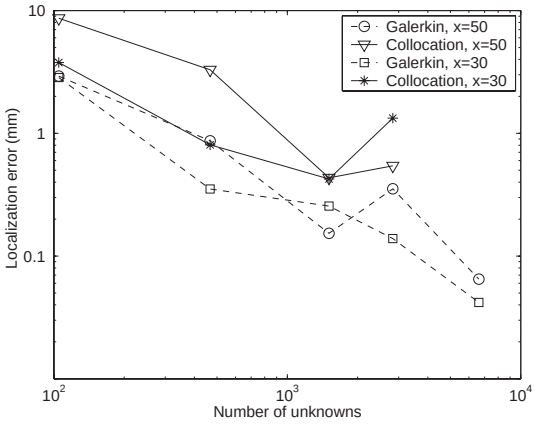

Figure 8: The localization error (mm) as a function of the number of unknowns for a dipole near the surface of the brain ($x = 50$) and for a dipole at the depth of 2.5 cm ($x = 30$) computed using the Galerkin and collocation methods with linear basis functions.

close to the triangles the Galerkin method improves the localization results significantly (Figures 8 and 9).

The large localization errors near the surface of the brain caused by improper discretization have resulted in the need to use the spherical model for the superficial sources. For example, Roth *et al.* [102] determined that the length of the sides of the triangles close to a dipolar source must be less than the distance to the source for accurate results. However, this problem can be alleviated significantly by using the Galerkin method with linear or higher order basis functions and with a sufficiently high number of surface elements. In Publication VI, the spatial variation of the relative errors for the Galerkin and the collocation methods with linear basis functions were compared. The results showed how the Galerkin method reduced the localization error near the surface of the brain (Figure 10).

The computational costs to obtain a given accuracy are less for the Galerkin method than for the collocation method. As the Galerkin method needs less unknowns to obtain the same accuracy than the collocation method, especially the solution time using the LU decomposition is shorter for the Galerkin method.

Increasing the number of surface elements increases the computation time. In the present thesis, this problem has been studied and sig-

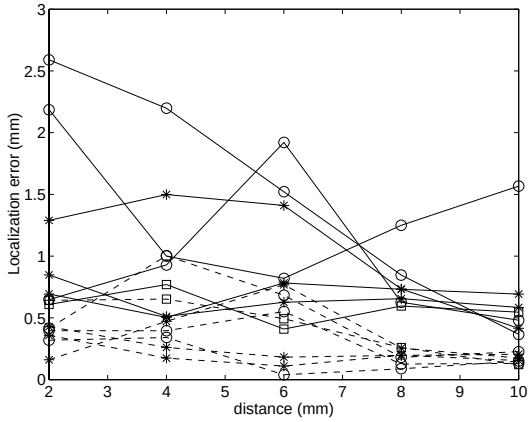

Figure 9: The localization error (mm) as a function of the distance from a triangle. The results are shown for dipoles under vertices (◦), center of the triangle (□), and midpoints of a triangle edge (*). Dashed lines refer to the Galerkin method and solid lines to the collocation method. There is a clear difference between the group of the Galerkin curves and the group of the collocation curves.

nificant progress could be obtained using the advanced iterative method with the precorrected-FFT method. However, the analytical computation of the magnetic field using the spherical model is so simple and fast that no numerical method can achieve the same speed. On the other hand, the forward problem solution using a realistically shaped conductor model is usually more accurate than that using a spherical model. The latter is reasonable only for superficial dipoles on brain regions of locally very spherical shape.

The simulations presented in Publication VI suggest that about 3 000 or more unknowns, i.e., more than 6 000 triangles, are needed for submillimeter localization accuracy caused by the inaccuracies in the brain shaped conductor model.

The author has observed that coarse discretization with constant potential approximation may cause local minima for the cost function [117], i.e. the relative error between the measured and computed magnetic fields that is minimized in the nonlinear search. The local minima emphasize the importance of good initial guesses and the requirements for the search algorithm. Using the Galerkin method with linear or higher order basis functions and a sufficiently large number of un-

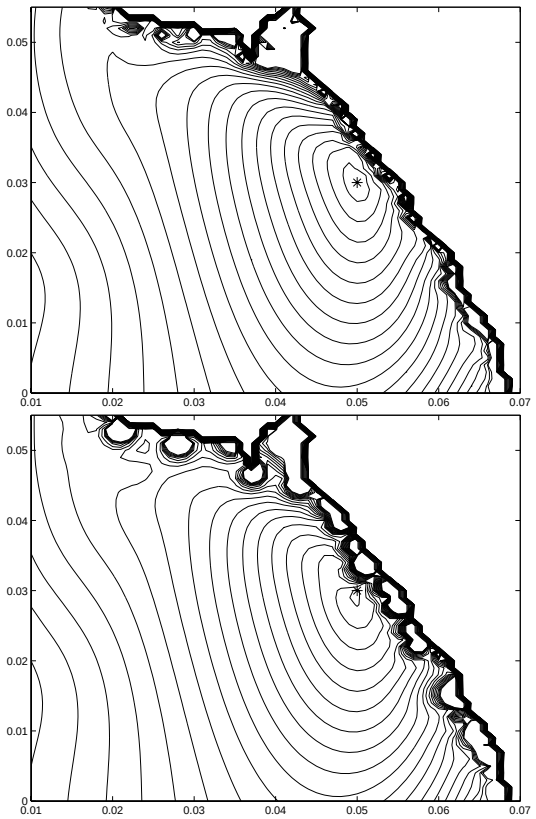

Figure 10: Simulated data for the spatial variation of the cost function, i.e. the relative error of the measured and computed magnetic fields, as a function of the guessed source dipole location. The source dipole for the simulated measurement data shown by star (*) is located near the surface of the brain in the temporal lobe. The upper figure is for the Galerkin method and the lower figure for the collocation method with linear basis functions. The coordinates are given in meters. The contours are drawn for relative errors between 0 to 1 with a step of 0.05. The white areas next to the surface indicate relative errors greater than 1. The size of the triangles of the conductor model is 7 mm.

knowns, the local minima problem may also be alleviated significantly as was done for the problem of large relative errors near the surface of the brain (Figure 10). In addition, new approaches have been explored to obtain the initial guesses [66, 129] and new optimization algorithms have been studied [123].

5.4 Other sources of error

In practise, there are several other sources of error, in addition to the conductor model and the computational methods. For example, the signal-to-noise ratio varies depending on the experiment and the corresponding neural sources. The source model may not be adequate for the actual neurophysiological sources. Especially, the correlated noise may cause severe localization errors. The noise from the device can be minimized by adjusting and calibrating the device.

Geometrical errors in the MR images must be removed by proper shimming of the MRI scanner. A good localization accuracy requires careful registration of MRI and MEG in which procedure the three head landmarks and the head position indicator coils [1] are digitized manually. The procedure is affected by interhuman variability.

During long neuromagnetic recordings the subject's head may move which easily destroys the localization accuracy. Thus, the subject's head must be supported properly and observed movements should be corrected. Recently, a method for observing and correction of head movements has been developed [125].

As discussed in Reference [95], several source models are needed to reliably localize, for example, epileptic sources in frontal lobes. Both dipolar and distributed source models are important, especially, for the localization of neural currents of pathophysiological phenomena as there is usually no a priori knowledge of the sources. To be able to restrict the distributed source model on the cortex, a realistically shaped conductor model is necessary.

6 Discussion

6.1 Remarks on the computational methods

It has commonly been thought that the Galerkin method is computationally too expensive for the bioelectromagnetic problems and is not worth implementing [65]. It has been known to be more accurate than the collocation method. In the present thesis, it has been shown that for the same accuracy the computational costs are smaller for the Galerkin method than for the collocation method. If only the solution time of the forward problem for a new dipole location is considered, computation time is shorter for the Galerkin method than for the collocation method, because a conductor model tesselated with less triangles can be used for the Galerkin method. In addition, the Galerkin method improves significantly the accuracy for dipoles near the surface of the brain.

The computation time could also be minimized using a locally refined triangular network [80, 137, 22]. However, the laborious computations, i.e., the calculation of the dense coefficient matrix and its LU decomposition or the preprocessing for the iterative method with the precorrected-FFT method, must be recomputed for each refined network. Especially, if the refining is carried out during the nonlinear search, the computation time increases drastically.

The Galerkin method with linear basis functions and the Bi-CGSTAB method with the precorrected-FFT method can be enlarged to be used for realistically shaped multilayer conductor models for EEG, MCG, and ECG. For EEG, the iterative method may be slow because of the poor conductivity of the skull. This potential problem may be eliminated by a new preconditioner or by performing multiple deflations.

The minimum current estimate needs a precise triangular network of the heavily convoluted cortex to obtain the normals of the cortex for anatomical constraints of the current orientations [124]. The computational methods studied here could also, in principle, employ such a precise conductor model instead of a smooth brain shaped envelope conductor model that includes the CSF in the fissures.

The effect of various computational and modelling methods must be studied separately for EEG and MEG. The error in the potential behaves differently from the error of the magnetic field as explained in Publication IV.

Inverse solution methods for finding focused or distributed current

sources which best explain the measured magnetic field are presented in Section 3.6. In all these methods, the forward problem needs to be solved either directly for a dipole or as a lead field for a unit dipole in fixed locations. Thus, the accuracy of the forward problem solution affects all source localization studies.

The numerical methods studied in this thesis were applied for the localization of early auditory responses originated in the brainstem [97]. A single dipole model was used. According to the electric recordings reported in the literature the measured responses are generated by two nearby sources. As a preliminary result from these studies it was concluded that the accurate computation of the forward solution allows for more complex source models, i.e. for successful localization the source model needs to describe accurately enough the underlying neurophysiological sources. To be able to obtain physiologically reasonable localization results various source models need to be applied.

6.2 Computation of transfer matrices

In References [87, 83] precomputed and stored transfer matrices have been presented to compute the magnetic field in the sensors directly without first solving the potential on the mesh. This method shortens significantly the computation time for each source location because the transfer matrix is smaller than the coefficient matrix for the unknown potential on the mesh. On the other hand the computer memory requirements may still be significant as the dense coefficient matrix must first be fully assembled to be able to form the transfer matrix. The transfer matrices cannot be used with the iterative solvers. However, the iterative method with the precorrected-FFT method can be used to compute the transfer matrix without forming the dense coefficient matrix. Thus, even for large problems the transfer matrix can be obtained quickly with minor memory requirements and the magnetic fields can be computed fast for each new dipole location.

As was presented in Table 1, the preprocessing time for the iterative solver with the precorrected-FFT method is significantly smaller than that of the LU decomposition. On the other hand, the iterative solution time is longer than the LU solution time for medium size meshes. Thus, when solving the forward problem for a small number of dipoles the iterative solver with the precorrected-FFT method is significantly more efficient than the LU decomposition as the preprocessing time dominates

in the total computation time. However, if several thousands of dipoles are solved the total iterative solution time starts to dominate. In this case the fastest approach is to use the transfer matrices which are obtained quickly by the iterative method with the precorrected-FTT method.

6.3 Computation of the lead fields

Some authors have suggested to solve the lead fields for a homogeneous dipole grid covering the whole brain region to overcome local minima and initial guess problems and to quickly localize the source with the realistically shaped conductor model [139, 26, 24]. In this approach, a large number of forward problem solutions are precomputed and stored in computer memory and the measured field is compared to these to find the source dipole. The precomputations must be performed for each realistically shaped conductor model and for each measurement configuration. The localization result is improved by interpolating the solutions of the forward problem for dipoles that are located between the grid dipoles. This approach could gain from the iterative method with the precorrected-FFT method as the lead fields can be computed accurately with small computer memory requirements. The lead fields of the superficial dipole locations could be computed using larger number of surface elements than for the deep dipole locations. Also the transfer matrix approach can be used.

Another approach to solve the forward problem quickly is to fit a sphere for each sensor of the MEG device so that the lead fields of the spheres approximate the lead fields of the dipole grid in the realistically shaped conductor model [26, 55] as the forward problem can be solved fast analytically for a sphere. Source localization becomes fast, but the approximation of the lead fields weakens the accuracy of the method.

The numerical methods studied in this thesis can also be used in the lead field analysis for EEG ([32, 29]) where the electric lead fields are obtained using the reciprocal approach.

In Reference [66], a multilayer perceptron is used in the MEG source localization to give an initial guess for a nonlinear minimization search or to localize the source quickly. The perceptron is trained by forward solutions for a large set of dipoles. The computational methods studied in the present thesis to compute the forward problem solutions could also be used to train the perceptron to give more accurate estimates for the initial guess or the final source location.

6.4 Isolated skull approach

The Isolated Skull Approach (ISA) was described by Hämäläinen and Sarvas [59]. It is used to improve the accuracy of the forward problem solutions for EEG by using the multilayer boundary element model for the head. Using the ISA, Hämäläinen and Sarvas showed in [59] that it is sufficient for MEG to use a brain shaped homogeneous conductor model.

Mosher *et al.* [83] used a three-layer spherical head model to compare the performance of the Galerkin and the collocation methods. Also the effect of the ISA was studied. Their conclusion was that the ISA improved the EEG results especially for superficial dipoles, but the ISA degraded the MEG results. In addition, though not mentioned in the paper, the results indicate that the improvement in the accuracy by the ISA was smallest for the Galerkin method with linear basis functions and largest for the collocation method with constant basis functions. For the collocation method with linear basis functions the use of the ISA degraded the EEG results for the deep sources.

Finke and Gulrajani [29] employed also a three-layer spherical head model with the ISA. They reported that when the skull conductivity was increased the accuracy of the potential on the outer surface was improved significantly when linear basis functions were used. The result was the opposite for constant basis functions. According to the authors the result was expected, since with linear basis functions the correction term in the ISA became more accurate together with the single layer solution. Constant basis functions were confirmed to be insufficient to model the rapid spatial changes of the potential on the tissue surfaces.

Thus, using more sophisticated potential modelling such as the Galerkin method with high-order basis functions the accuracy of the potential on the outer surface of the head can be improved using the ISA. On the other hand, basing on the observations from the results in Reference [83] it can be expected that the effect of the ISA will be smaller for sophisticated potential modelling and fine meshes. If recently obtained higher values for the conductivity of the skull [38, 93, 70] are used, the effect of the ISA will be reduced more. The effect of the ISA in MEG should be investigated further.

Because the skull and scalp are thin, proper modelling of the potential and the geometry is needed in order to obtain accurately the potential on the outer surface. For three layer models, the size of the elements should be chosen carefully taking into account the thickness of

the layers. The small effect of the skull and the scalp on MEG source localization using the state of the art boundary element modelling should be studied accurately.

6.5 Coupled finite and boundary element modelling

As long as the conductivity of the brain tissue can be assumed to be isotropic and homogeneous, the boundary element method can be used to solve the integral equation (12). If the conductivity distribution is taken into account the finite difference method (FDM) or the finite element method (FEM) must be used. These methods are employed in various bioelectric field problems [65]. A comparison of the methods in EEG and MEG was reported by Pruis *et al.* [100]. It is important to note that the BEM and the FEM approaches are computationally quite different as the coefficient matrix is dense in the BEM and sparse in the FEM approach and the number of elements is usually significantly smaller for the BEM than for the FEM.

Haueisen *et al.* [52, 53] reported that the inhomogeneous brain conductivity does not essentially affect the localization of the MEG recordings, but it has a notable impact on the localization of the EEG recordings. The anisotropy of the conductivity was found to affect mainly on the MEG source strength estimation. The effect of the skull on the EEG recordings is especially significant. The local variations of the thickness of the skull and the complicated conductivity distribution of the skull need to be modelled carefully to improve the EEG source localization accuracy [92, 71]. The finite element modelling is needed for the individual skull conductivity distribution. As the exact data for the conductivity distribution is not available, the precise modelling of the skull thickness in the multilayer BEM modelling may increase the EEG source localization accuracy. The iterative method with the precorrected-FFT method, studied in the present thesis for MEG, would be worth trying also for EEG.

Bradley *et al.* presented a hybrid head model where the brain was modeled by the BEM and the skull and the scalp by the BEM or the FEM [14]. They reported that for low skull conductivities the potential on the scalp can be obtained more accurately using the FEM for the skull and the scalp than using the BEM for all layers or for the brain and the scalp. However, for individual volume conductor models the skull and the scalp may be difficult to model with the FEM because they are thin

layers. A hybrid model where the brain is modelled by the FEM and the skull and the scalp by the BEM, could be used to study the effect of the anisotropy of the brain tissue on the source localization. The numerical methods studied in the present thesis would be useful as the number of unknowns will be large.

7 Conclusions

The present thesis consists of three parts that apply anatomical information and advanced computational methods for the neuromagnetic source localization. In the first part, neuromagnetic source localization results were combined with individual anatomical information on three-dimensional MR reconstructions of the subject's brain. Applying this technique, new significant information was obtained about the continuity of visual perception during eyeblinks in humans. Visualization of localization results on MR reconstructions has become a common practice in the field of bioelectromagnetism.

Individual anatomical information can also be used to form realistically shaped volume conductor models in order to improve the neuromagnetic source localization accuracy. In the second part of this thesis, it was shown that the whole head MEG with individual brain shaped conductor models can be used to study the cognitive processes associated to deep brain structures like memory associated to the hippocampus. In spite of the more accurate localization results, the realistically shaped conductor model has not replaced the simple spherical model. In practise, mainly three problems have decreased the interest in the everyday use of the realistically shaped conductor model. First, MR images must be obtained for each subject, increasing the costs of the studies. Second, a specialized software and some expertise are needed to form the realistically shaped conductor model. Third, the use of the realistically shaped conductor model is computationally more costly than to apply the spherical model.

In the third part of the thesis, advanced computational methods were studied to facilitate the use of realistically shaped conductor models in neuromagnetic source localization. As a first application, the methods were tested with unit spheres and then applied to brain shaped homogeneous conductor models using a single current dipole. The accuracy of the forward problem solution, especially near the surface of the conductor model, could be significantly improved using the Galerkin method with linear basis functions. Contrary to a common expectation, the Galerkin method was shown to be efficient and even faster than the widely used collocation method with linear basis functions for a given forward solution accuracy. Large problems could be solved quickly without the explicit formation of the dense matrix with small computer

memory requirements using the iterative Bi-CGSTAB method with the precorrected-FFT method.

The solution of the neuromagnetic integral equation was an interesting application for the advanced iterative methods with the precorrected-FFT method not only in the field of the bioelectromagnetism but also in the numerical mathematics of integral equations.

The methods studied can be applied for MEG, EEG, MCG or ECG with multicompartment volume conductor models and with focused or distributed current source models. The forward problem solution is needed in all bioelectromagnetic source localization. The methods can be taken into routine use for neuromagnetic source localization to improve the source localization accuracy and to decrease the computational costs of accurate modelling.

Employing the anisotropic conductivity distribution of the brain obtained by MRI is one of the future challenges in the neuromagnetic source analysis. The FEM approach must be used in order to model the anisotropic conductivity distribution. The computational costs of the FEM may be larger than for the BEM. Especially, the region exterior to the head must also be discretized in the FEM modeling. This work can be avoided by using a hybrid head model, i.e. the BEM model for the skull and the scalp and the FEM model for the brain. The numerical methods studied in the present thesis, can be applied in the hybrid approach.

References

[1] S. Ahlfors and R. J. Ilmoniemi. Magnetometer position indicator for multichannel MEG. In S. J. Williamson, M. Hoke, G. Stroink, and M. Kotani, editors, *Advances in biomagnetism*, pages 693–696, New York, 1989. Plenum Press.

[2] J. F. Ahner and R. F. Arenstrof. On the eigenvalues of the electrostatic integral operator. *J. Math. Anal. Appl.* **117**, 187–197, 1986.

[3] A. I. Ahonen, M. S. Hämäläinen, M. J. Kajola, J. E. T. Knuutila, P. P. Laine, O. V. Lounasmaa, L. T. Parkkonen, J. T. Simola, and C. D. Tesche. A 122-channel SQUID instrument for investigating the magnetic signals from the human brain. *Physica Scripta* **T49**, 198–205, 1993.

[4] W. Andrä and H. Nowak, editors. *Magnetism in Medicine*. Wiley VCH, Berlin, 1998.

[5] S. Baillet and L. Garnero. A bayesian approach to introducing anatomo-functional priors in the EEG/MEG inverse problem. *IEEE Trans. Biomed. Eng.* **44**, 373–385, 1997.

[6] S. Baillet, J. C. Mosher, and R. M. Leahy. Electromagnetic brain mapping. *IEEE Signal Processing Magazine* **18**, 14–30, 2001.

[7] A. C. L. Barnard, I. M. Duck, M. S. Lynn, and W. P. Timlake. The application of electromagnetic theory to electrocardiography. II. numerical solution of the integral equations. *Biophys. J.* **7**, 463–491, 1967.

[8] R. Barrett et al. *Templates for the Solution of Linear Systems: Building Blocks for Iterative Methods*. SIAM, Philadelphia, 1993.

[9] D. S. Barth, W. Sutherling, J. Broffman, and J. Beatty. Magnetic localization of a dipolar current source implanted in a sphere and a human cranium. *Electroenceph. Clin. Neurophys.* **63**, 260–273, 1986.

[10] D. S. Barth, W. Sutherling, J. Engel, Jr., and J. Beatty. Neuromagnetic localization of epileptiform spike activity in the human brain. *Science* **218**, 891–894, 1982.

[11] J. W. Belliveau, D. N. Kennedy, R. C. McKinstry, B. R. Buchbinder, R. M. Weisskoff, M. S. Cohen, J. M. Vevea, T. J. Brady, and B. R. Rosen. Functional mapping of the human visual cortex by magnetic resonance imaging. *Science* **254**, 716–719, 1991.

[12] P. Berg and M. Davies. Eyeblink-related potentials. *Electroenceph. Clin. Neurophys.* **69**, 1–5, 1988.

[13] C. Bertrand, M. Ohmi, R. Suzuki, and H. Kado. A probabilistic solution to the MEG inverse problem via MCMC methods: the reversible jump and parallel tempering algorithms. *IEEE Trans. Biomed. Eng.* **48**, No. 5, 533–542, 2001.

[14] C. P. Bradley, G. M. Harris, and A. J. Pullan. The computational performance of a high-order coupled FEM/BEM procedure in electropotential problems. *IEEE Trans. Biomed. Eng.* **48**, No. 11, 1238–1250, 2001.

[15] D. Brenner, J. Lipton, L. Kaufman, and S. J. Williamson. Somatically evoked magnetic fields of the human brain. *Science* **199**, 81–83, 1978.

[16] D. Brenner, S. J. Williamson, and L. Kaufman. Visually evoked magnetic fields of the human brain. *Science* **190**, 480–482, 1975.

[17] J. Budiman and D. S. Buchanan. An alternative to the biomagnetic forward problem in a realistically shaped head model, the "weighted vertices". *IEEE Trans. Biomed. Eng.* **40**, 1048–1053, 1993.

[18] G. Chen and J. Zhou. *Boundary Element Methods.* Academic Press, London, 1992.

[19] L. P. Clarke, R. P. Velthuizen, M. A. Camacho, J. J. Heine, M. Vaidyanathan, L. O. Hall, R. W. Thatcher, and M. L. Silbiger. MRI segmentation: Methods and applications. *Magn. Reson. Imaging* **13**, 343–368, 1995.

[20] A. Crouzeix, B. Yvert, O. Bertrand, and J. Pernier. An evaluation of dipole reconstruction accuracy with spherical and realistic head models in MEG. *Clin. Neurophy.* **110**, 2176–2188, 1999.

[21] B. N. Cuffin. Effects of head shape on EEG's and MEG's. *IEEE Trans. Biomed. Eng.* **37**, No. 1, 44–52, 1990.

[22] B. N. Cuffin. A method for localizing EEG sources in realistic head models. *IEEE Trans. Biomed. Eng.* **42**, 68–71, 1995.

[23] J. C. de Munck. A linear discretization of the volume conductor boundary integral equation using analytically integrated elements. *IEEE Trans. Biomed. Eng.* **39**, 986–990, 1992.

[24] J. C. de Munck, A. de Jongh, and B. W. van Dijk. The localization of spontaneous brain activity: An efficient way to analyze large data sets. *IEEE Trans. Biomed. Eng.* **48**, No. 11, 1221–1228, 2001.

[25] J. C. de Munck, B. W. van Dijk, and H. Spekreijse. Mathematical dipoles are adequate to describe realistic generators of human brain activity. *IEEE Trans. Biomed. Eng.* **35**, 960–966, 1988.

[26] J. J. Ermer, J. C. Mosher, S. Baillet, and R. M. Leahy. Rapidly recomputable EEG forward models for realistic head shapes. *Phys. Med. Biol.* **46**, No. 4, 1265–1282, 2001.

[27] A. S. Ferguson and G. Stroink. Factors affecting the accuracy of the boundary element method in the forward problem — I: Calculating surface potentials. *IEEE Trans. Biomed. Eng.* **44**, 1139–1155, 1997.

[28] A. S. Ferguson, X. Zhang, and G. Stroink. A complete linear discretization for calculating the magnetic field using the boundary element method. *IEEE Trans. Biomed. Eng.* **41**, 455–460, 1994.

[29] S. Finke and R. M. Gulrajani. Conventional and reciprocal approaches to the forward problem of electroencephalography. *Electromagnetics* **21**, 513–530, 2001.

[30] G. Fischer, B. Tilg, P. Wach, G. Lafer, and W. Rucker. Analytical validation of the BEM — application of BEM to the electrocardiographic forward and inverse problem. *Computer Methods and Programs in Biomedicine* **55**, 99–106, 1998.

[31] G. Fischer, B. Tilg, P. Wach, R. Modre, U. Leder, and H. Nowak. Application of high-order boundary elements to the electrocardiographic inverse problem. *Computer Methods and Programs in Biomedicine* **58**, No. 2, 119–131, 1999.

[32] D. J. Fletcher, A. Amir, D. L. Jewett, and G. Fein. Improved method for computation of potentials in a realistic head shape model. *IEEE Trans. Biomed. Eng.* **42**, 1094–1104, 1995.

[33] R. W. Freund and N. M. Nachtigal. QMR: a quasi-minimal residual method for non-Hermitian linear systems. *Numerische Math.* **60**, 315–339, 1991.

[34] J. H. M. Frijns, S. L. de Snoo, and R. Schoonhoven. Improving the accuracy of the boundary element method by the use of second-order interpolation functions. *IEEE Trans. Biomed. Eng.* **47**, 1336–1346, 2000.

[35] M. Fuchs, R. Drenckhahn, H.-A. Wiscgmann, and M. Wagner. An improved boundary element method for realistic volume-conductor modeling. *IEEE Trans. Biomed. Eng.* **45**, No. 8, 980–997, 1998.

[36] M. Fuchs, J. Kastner, M. Wagner, S. Hawes, and J. S. Ebersole. A standardized boundary element method volume conductor model. *Clin. Neurophysiol.* **113**, No. 5, 702–712, 2002.

[37] C. Gallen, D. Sobel, T. Waltz, M. Aung, B. Copeland, B. Schwartz, E. Hirschkoff, and F. Bloom. Noninvasive presurgical neuromagnetic mapping of somatosensory cortex. *Neurosurgery* **33**, 260–268, 1993.

[38] L. A. Geddes and L. E. Baker. The specific resistance of biological material – a compendium of data for the biomedical engineering and physiologist. *Med. Biol. Eng.* **5**, 271–293, 1967.

[39] N. G. Gençer and I. O. Tanzer. Forward problem solution of electromagnetic source imaging using a new BEM formulation with high-order elements. *Phys. Med. Biol.* **44**, 2275–2287, 1999.

[40] D. B. Geselowitz. On bioelectric potentials in an inhomogeneous volume conductor. *Biophys. J.* **7**, 1–11, 1967.

[41] D. B. Geselowitz. On the magnetic field generated outside an inhomogeneous volume conductor by internal current sources. *IEEE Trans. Magn.* **MAG-6**, 346–347, 1970.

[42] G. Golub and C. van Loan. *Matrix Computations*. Johns Hopkins University Press, Baltimore, 2nd edition, 1989.

[43] L. Greengard and V. Rokhlin. A fast algorithm for particle simulations. *J. Comp. Phys.* **73**, 325–348, 1987.

[44] E. Halgren, T. Raij, K. Marinkovic, V. Jousmäki, and R. Hari. Cognitive response profile of the human fusiform face area as determined by MEG. *Cerebral Cortetx* **10**, 69–81, 2000.

[45] H. A. Haque, T. Musha, and M. Nakajima. Three-shell head model constructed from scalp geometry for electroencephalogram dipole localization. *Front. Med. Biol. Eng.* **9**, 295–304, 1999.

[46] R. Hari, K. Aittoniemi, M.-L. Järvinen, T. Katila, and T. Varpula. Auditory evoked transient and sustained magnetic fields of the human brain: Localization of the neural generators. *Exp. Brain Res.* **40**, 237–240, 1980.

[47] R. Hari, N. Forss, S. Avikainen, E. Kirveskari, S. Salenius, and G. Rizzolatti. Activation of human primary motor cortex during action observation: a neuromagnetic study. *Proc. Natl. Acad. Sci. USA* **95**, 15061–15065, 1998.

[48] R. Hari, M. Hämäläinen, E. Kaukoranta, J. Mäkelä, S.-L. Joutsiniemi, and J. Tiihonen. Selective listening modifies activity of the human auditory cortex. *Exp. Brain Res.* **74**, 463–470, 1989.

[49] R. Hari, S.-L. Joutsiniemi, and J. Sarvas. Spatial resolution of neuromagnetic records: theoretical calculations in a spherical model. *Electroenceph. Clin. Neurophys.* **71**, 64–72, 1988.

[50] R. Hari, E. Kaukoranta, K. Reinikainen, T. Huopaniemi, and J. Mauno. Neuromagnetic localization of cortical activity evoked by painful dental stimulation in man. *Neurosci. Lett.* **42**, 77–82, 1983.

[51] R. Hari, S. Levänen, and T. Raij. Timing of human cortical functions during cognition: role of MEG. *Trends in Cognitive Sciences* **4**, No. 12, 455–462, 2000.

[52] J. Haueisen, C. Ramon, M. Eiselt, H. Brauer, and H. Nowak. Influence of tissue resistivities on neuromagnetic fields and electric potentials studied with a finite element model of the head. *IEEE Trans. Biomed. Eng.* **44**, No. 8, 727–735, 1997.

[53] J. Haueisen, D. S. Tuch, C. Ramon, P. H. Schimpf, V. J. Wedeen, J. S. George, and J. W. Belliveau. The influence of brain tissue anisotropy on human EEG and MEG. *NeuroImage* **15**, 159–166, 2002.

[54] B. He, T. Musha, Y. Okamoto, S. Homma, Y. Nakajima, and T. Sato. Electric dipole tracing in the brain by means of the boundary element method and its accuracy. *IEEE Trans. Biomed. Eng.* **BME-34**, No. 6, 406–414, 1987.

[55] M. X. Huang, J. C. Mosher, and R. M. Leahy. A sensor-weighted overlapping-sphere head model and exhaustive head model comparison for MEG. *Phys. Med. Biol.* **44**, 423–440, 1999.

[56] M. Hämäläinen. Anatomical correlates for magnetoencephalography: integration with magnetic resonance images. *Clin. Phys. Physiol. Meas.* **12**, 29–32, 1991.

[57] M. Hämäläinen, R. Hari, R. J. Ilmoniemi, J. Knuutila, and O. V. Lounasmaa. Magnetoencephalography — theory, instrumentation, and applications to noninvasive studies of the working human brain. *Rev. Mod. Phys.* **65**, 413–497, 1993.

[58] M. Hämäläinen and J. Nenonen. Magnetic source imaging. In J. Webster, editor, *Encyclopedia of Electrical Engineering*, volume 12, pages 133–148. Wiley & Sons, New York, 1999.

[59] M. Hämäläinen and J. Sarvas. Realistic conductivity geometry model of the human head for interpretation of neuromagnetic data. *IEEE Trans. Biomed. Eng.* **36**, No. 2, 165–171, 1989.

[60] M. S. Hämäläinen. Functional localization based on measurements with a whole-head magnetometer system. *Brain Topography* **7**, No. 4, 283–289, 1995.

[61] M. S. Hämäläinen and R. J. Ilmoniemi. Interpreting magnetic fields of the brain: minimum norm estimates. *Med. & Biol. Eng. & Comput.* **32**, 35–42, 1994.

[62] M. S. Hämäläinen and J. T. Nenonen. Magnetic source imaging. In P. J. Lee, editor, *Engineering Superconductivity*, pages 464–479. Wiley & Sons, New York, 2001.

[63] M. S. Hämäläinen and J. Sarvas. Feasibility of the homogeneous head model in the interpretation of neuromagnetic fields. *Phys. Med. Biol.* **32**, No. 1, 91–97, 1987.

[64] R. J. Jaszczak. Tomographic radiopharmaceutical imaging. *Proc. IEEE* **76**, 1079–1094, 1988.

[65] C. R. Johnson. Computational and numerical methods for bioelectric field problems. *Critical Reviews in Biomedical Engineering* **25**, 1–81, 1997.

[66] S. C. Jun, B. A. Pearlmutter, and G. Nolte. Fast accurate MEG source localization using a multilayer perceptron trained with real brain noise. *Phys. Med. Biol.* **47**, 2547–2560, 2002.

[67] V. O. Kelhä, J. M. Pukki, R. S. Peltonen, A. J. Penttinen, R. J. Ilmoniemi, and J. J. Heino. Design, construction, and performance of a large-volume magnetic shield. *IEEE Trans. Magn.* **MAG-18**, 260–270, 1982.

[68] G. F. Knoll. Single-photon emission computed tomography. *Proc. IEEE* **71**, 320–329, 1983.

[69] S. W. Kuffler, J. G. Nicholls, and A. R. Martin. *From Neuron to Brain, A Cellular Approach to the Function of the Nervous System.* Sinauer Accociates, Sunderland, 2nd edition, 1984.

[70] S. K. Law. Thickness and resistivity variations over the upper surface of the human skull. *Brain Topogr.* **6**, 99–109, 1993.

[71] R. M. Leahy, J. C. Mosher, M. E. Spencer, M. X. Huang, and J. D. Lewine. A study of dipole localization accuracy for MEG and EEG using a human skull phantom. *Electroenceph. Clin. Neurophys.* **107**, 159–173, 1998.

[72] R. R. Llinas, U. Ribary, D. Jeanmonod, E. Kronberg, and P. P. Mitra. Thalamocortical dysrhythmia: A neurological and neuropsychiatric syndrome charaterized by magnetoencephalography. *Proc. Natl. Acad. Sci. USA* **96**, 15222–15227, 1999.

[73] S.-T. Lu, M. S. Hämäläinen, R. Hari, R. J. Ilmoniemi, O. V. Lounasmaa, M. Sams, and V. Vilkman. Seeing faces activates three separate areas outside the occipital visual cortex in man. *Neurosci.* **43**, 287–290, 1991.

[74] M. S. Lynn and W. P. Timlake. The use of multiple deflations in the numerical solution of singular systems of equations, with applications to potential theory. *SIAM J. Numer. Anal.* **5**, 303–322, 1968.

[75] J. Lötjönen. *Construction of Boundary Element Models in Bioelectromagnetism.* PhD thesis, Helsinki University of Technology, 2000.

[76] J. Lötjönen, P.-J. Reissman, I. E. Mangin, and T. Katila. Model extraction from magnetic resonance volume data using a deformable pyramid. *Medical Image Analysis* **3**, 387–406, 1999.

[77] D. Marquart. An algorithm for least-squares estimation of nonlinear parameters. *J. Soc. Indust. Appl. Math.* **11**, 431–441, 1963.

[78] J. W. H. Meijs, F. G. C. Bosch, M. J. Peters, and F. H. Lopes da Silva. On the magnetic field distribution generated by a dipolar current source situated in a realistically shaped compartment model of the head. *Electroenceph. Clin. Neurophys.* **66**, 286–298, 1987.

[79] J. W. H. Meijs, B. J. ten Voorde, M. J. Peters, C. J. Stok, and F. H. Lopes da Silva. The influence of various head models on EEG's and MEG's. In G. Pfurtscheller and F. H. Lopes da Silva, editors, *Functional Brain Imaging*, pages 31–46, Toronto, 1988. Huber.

[80] J. W. H. Meijs, O. W. Weier, M. J. Peters, and A. van Oosterom. On the numerical accuracy of the boundary element method. *IEEE Trans. Biomed. Eng.* **36**, No. 10, 1038–1049, 1989.

[81] E. Menninghaus and B. Lütkenhöner. Localization of a dipolar source in a skull phantom: Realistic versus spherical model. *IEEE Trans. Biomed. Eng.* **41**, 986–989, 1994.

[82] I. Merlet, L. Garcia-Larrea, P. Ryvlin, J. Isnard, M. Sindou, and F. Mauguière. Topographical reliability of mesio-temporal sources of interictal spikes in temporal lobe epilepsy. *Electroenceph. Clin. Neurophys.* **107**, 206–212, 1998.

[83] J. C. Mosher, R. M. Leahy, and P. S. Lewis. EEG and MEG: Forward solutions for inverse problems. *IEEE Trans. Biomed. Eng.* **46**, 245–259, 1999.

[84] J. C. Mosher and P. S. Lewis. Multiple dipole modelling and localization from spatio-temporal MEG data. *IEEE Trans. Biomed. Eng.* **39**, 541–557, 1992.

[85] J. P. Mäkelä, E. Kirveskari, M. Seppä, M. Hämäläinen, N. Forss, S. Avikainen, O. Salonen, S. Salenius, T. Kovala, T. Randell, J. Jääskeläinen, and R. Hari. Three-dimensional integration of

brain anatomy and function to facilitate intraoperative navigation around the sensorimotor strip. *Hum. Brain Mapp.* **12**, 180–192, 2001.

[86] J. Nenonen, R. J. Ilmoniemi, and T. Katila, editors. *Biomag2000, Proceedings of the 12th International Conference on Biomagnetism*, Espoo, Finland, 2001. Helsinki University of Technology, Laboratory of Biomedical Engineering.

[87] J. Nenonen, C. J. Purcell, B. M. Horacek, G. Stroink, and T. Katila. Magnetocardiographic functional localization using a current dipole in a realistic torso. *IEEE Trans. Biomed. Eng.* **38**, No. 7, 658–664, 1991.

[88] N. Nishitani and R. Hari. Viewing lip forms: Cortical dynamics. *Neuron* **36**, 1211–1220, 2002.

[89] H. Nowak, J. Haueisen, F. Giessler, and R. Huonker, editors. *Biomag2002, Proceedings of the 13th International Conference on Biomagnetism, Jena, Germany*, Berlin, 2002. VDE Verlag.

[90] P. L. Nunez. *Electric Fields of the Brain: The Neurophysics of EEG*. Oxford University Press, New York, 1981.

[91] R. Näätänen, A. Lehtokokski, M. Lennes, M. Cheour, M. Huotilainen, A. Iivonen, M. Vainio, P. Alku, R. Ilmoniemi, A. J. A. Luuk, J. Sinkkonen, and K. Alho. Language-specific phoneme representations revealed by electric and magnetic brain responses. *Nature* **385**, 432–434, 1997.

[92] J. Ollikainen, M. Vauhkonen, P. A. Karjalainen, and J. P. Kaipio. Effects of local skull inhomogenities on EEG source estimation. *Med. Eng. Phys.* **21**, 143–154, 1999.

[93] T. F. Oostendorp, J. Delbeke, and D. F. Stegeman. The conductivity of the human skull: Results of *in vivo* and *in vitro* measurements. *IEEE Trans. Biomed. Eng.* **47**, No. 11, 1487–1492, 2000.

[94] T. F. Oostendorp and A. van Oosterom. Source parameter estimation in inhomogeneous volume conductors of arbitrary shape. *IEEE Trans. Biomed. Eng.* **36**, 382–391, 1989.

[95] P. Ossenblok, M. Fuchs, D. N. Velis, E. Veltman, J. P. Pijn, and F. H. L. da Silva. Source analysis of lesional frontal-lobe epilepsy. *IEEE Eng. Med. Biol.* **18**, 67–77, 1999.

[96] R. Paetau, M. Kajola, and R. Hari. Magnetoencephalography in the study of epilepsy. *Neurophysiol. Clin.* **20**, 169–187, 1990.

[97] L. Parkkonen and J. Mäkelä. MEG sees deep sources: Measuring and modelling brainstem auditory evoked fields. In H. Nowak, J. Haueisen, F. Giessler, and R. Huonker, editors, *Proceedings of the 13th International Conference on Biomagnetism, Jena, Germany*, pages 107–109, Berlin, 2002. VDE Verlag.

[98] J. R. Phillips and J. K. White. A precorrected-FFT method for electrostatic analysis of complicated 3-D structures. *IEEE Trans. Computer-Aided Design* **16**, No. 10, 1059–1072, 1997.

[99] R. Plonsey. *Biomagnetic Phenomena*. McGraw-Hill, New York, 1969.

[100] G. W. Pruis, B. H. Gilding, and M. J. Peters. A comparison of different numerical methods for solving the forward problem in EEG and MEG. *Physiol. Meas.* **14**, A1–A9, 1993.

[101] J. J. Riera and M. E. Fuentes. Electric lead field for a piecewise homogeneous volume conductor model of the head. *IEEE Trans. Biomed. Eng.* **45**, No. 6, 746–753, 1998.

[102] B. J. Roth, M. Balish, A. Gorbach, and S. Sato. How well does a three-sphere model predict positions of dipoles in a realistically shaped head? *Electroenceph. Clin. Neurophys.* **87**, 175–184, 1993.

[103] Y. Saad and M. H. Schultz. GMRES: a generalized minimal residual algorithm for solving nonsymmetric linear systems. *SIAM J. Sci. Stat. Comput.* **7**, 856–869, 1986.

[104] R. Salmelin, E. Service, P. Kiesilä, K. Uutela, and O. Salonen. Impared perception of visual word form in dyslexia revealed with magnetoencephalography. *Annals of Neurology* **40**, 157–162, 1996.

[105] M. Sams, R. Aulanko, M. Hämäläinen, R. Hari, O. V. Lounasmaa, S.-T. Lu, and J. Simola. Seeing speech: visual information from lip movements modifies activity in the human auditory cortex. *Neurosci. Lett.* **127**, 141–145, 1991.

[106] J. Sarvas. Basic mathematical and electromagnetic concepts of the biomagnetic inverse problem. *Phys. Med. Biol.* **32**, 11–22, 1987.

[107] H. A. Schlitt, L. Heller, R. Aaron, E. Best, and D. M. Ranken. Evaluation of boundary element methods for the EEG forward problem: Effect of linear interpolation. *IEEE Trans. Biomed. Eng.* **42**, 52–58, 1995.

[108] U. Schmitt, A. K. Louis, F. Darvas, H. Buchner, and M. Fuchs. Numerical aspects of spatio-temporal current density reconstruction from EEG-/MEG-data. *IEEE Trans. Med. Imag.* **20**, No. 4, 314–324, 2001.

[109] I. H. Sloan. Error analysis of boundary integral methods. In *Acta Numerica*, pages 287–339. Cambridge University Press, 1992.

[110] J. Talairach and P. Tournoux. *Co-planar stereotaxic atlas of the human brain*. Thieme, Stuttgart, 1984.

[111] C. E. Tenke, C. E. Schroeder, J. C. Arezzo, and H. G. Vaughan. Interpretation of high-resolution current source density profiles: A simulation of sublaminar contributions to the visual evoked potential. *Exp. Brain Res.* **94**, 183–192, 1993.

[112] C. D. Tesche and J. Karhu. Somatosensory evoked magnetic fields arising from sources in the human cerebellum. *Brain Res.* **744**, 23–31, 1997.

[113] C. D. Tesche and J. Karhu. Theta oscillations index human hippocampal activation during a working memory task. *Proc. Natl. Acad. Sci. USA* **97**, 919–924, 2000.

[114] R. F. Thompson. *The Brain, An Introduction to Neuroscience*. Freeman, New York, 1985.

[115] J. Tiihonen, M. Kajola, and R. Hari. Magnetic mu rhythm in man. *Neurosci.* **32**, 793–800, 1989.

[116] A. N. Tikhonov and V. Y. Arsenin. *Solutions of Ill-Posed Problems*. Winston & Sons, Washington DC, 1977.

[117] S. Tissari. Realistically shaped conductor model in magnetoencephalography. Licentiate's thesis, Helsinki University of Technology, Espoo, Finland, 1994.

[118] S. Tomita, S. Kajihara, Y. Kondo, Y. Yoshida, K. Shibata, and H. Kado. Influence of head model in biomagnetic source localication. *Brain Topogr.* **8**, 337–340, 1996.

[119] J. H. Tripp. Physical concepts and mathematical models. In S. Williamson *et al.*, editor, *Biomagnetism, An Interdisciplinary Approach*, pages 101–139, New York, 1983. Plenum Press.

[120] D. S. Tuch, V. J. Wedeen, A. M. Dale, J. S. George, and J. W. Belliveau. Conductivity mapping of biological tissue using diffusion MRI. *Ann. NYAS* **888**, 314–316, 1999.

[121] L. Urankar. Common compact analytical formulas for computation of geometry integrals on a basic cartesian sub-domain in boudary and volume integral methods. *Eng. Anal. Bound. Elem.* **7**, No. 3, 124–129, 1990.

[122] M. A. Uusitalo and R. J. Ilmoniemi. Signal-space projection method for separating MEG or EEG into components. *Med. & Biol. Eng. & Comput.* **35**, 135–140, 1997.

[123] K. Uutela, M. Hämäläinen, and R. Salmelin. Global optimization in the localization of neuromagnetic sources. *IEEE Trans. Biomed. Eng.* **45**, No. 6, 716–723, 1998.

[124] K. Uutela, M. Hämäläinen, and E. Somersalo. Visualization of magnetoencephalographic data using minimum current estimates. *NeuroImage* **10**, 173–180, 1999.

[125] K. Uutela, S. Taulu, and M. Hämäläinen. Detecting and correcting for head movements in neuromagnetic measurements. *NeuroImage* **14**, 1424–1431, 2001.

[126] H. van der Vorst. Bi-CGSTAB: A fast and smoothly converging variant of Bi-CG for the solution of nonsymmetric linear systems. *SIAM J. Sci. Stat. Comput.* **13**, 631–644, 1992.

[127] A. van Oosterom and J. Strackee. The solid angle of a plane triangle. *IEEE Trans. Biomed. Eng.* **30**, 125–126, 1983.

[128] D. van 't Ent, J. C. de Munck, and A. L. Kaas. A fast method to derive realistic BEM models for E/MEG source reconstruction. *IEEE Trans. Biomed. Eng.* **48**, No. 12, 1434–1443, 2001.

[129] G. Van Hoey, J. De Clerq, B. Vanrumste ad R. Van de Walle, I. Limahieu, M. D'Havé, and P. Boon. EEG dipole source localization using artificial neural networks. *Phys. Med. Biol.* **45**, 997–1011, 2000.

[130] A. Villringer and B. Chance. Non-invasive optical spectroscopy and imaging of human brain function. *Trends Neurosci.* **20**, No. 10, 435–442, 1997.

[131] H. von Helmholtz. Ueber einige Gesetze der Vertheilung elektrischer Ströme in körperlichen Leitern, mit Anwendung auf die thrierisch-elektrischen Versuche. *Ann. Phys. Chem.* **89**, 211–233, 353–377, 1853.

[132] P. Wach, B. Tilg, G. Lafer, and W. Rucker. Magnetic source imaging in the human heart: estimating cardiac electrical sources from simulated and measured magnetocardiogram data. *Med. & Biol. Eng. & Comput.* **35**, 157–166, 1997.

[133] H. Weinberg, P. Brickett, F. Coolsma, and M. Baff. Magnetic localization of intracranial dipoles: Simulation with a physical model. *Electroenceph. Clin. Neurophys.* **64**, 159–170, 1986.

[134] S. J. Williamson and L. Kaufman. Biomagnetism. *J. Magn. Magn. Mat.* **22**, 129–201, 1981.

[135] S. J. Williamson, J.-Z. Wang, and R. J. Ilmoniemi. Method for locating sources of human alpha activity. In S. J. Williamson, M. Hoke, G. Stroink, and M. Kotani, editors, *Advances in biomagnetism*, pages 257–260, New York, 1989. Plenum Press.

[136] A. B. Wolbarst. *Physics of radiology*. Prentice Hall International, 2000.

[137] B. Yvert, O. Bertrand, J. F. Echallier, and J. Pernier. Improved forward EEG calculations using local mesh refinement of realistic head geometries. *Electroenceph. Clin. Neurophys.* **95**, 381–392, 1995.

[138] B. Yvert, O. Bertrand, M. Thévenet, J. F. Echallier, and J. Pernier. A systematic evaluation of the spherical model accuracy in EEG dipole localization. *Electroenceph. Clin. Neurophys.* **102**, 452–459, 1997.

[139] B. Yvert, A. Crouzeix-Cheylus, and J. Pernier. Fast realistic modeling in bioelectromagnetism using lead-field interpolation. *Human Brain Mapping* **14**, 48–63, 2001.

[140] J. E. Zimmerman, P. Thiene, and J. T. Harding. Design and operation of stable RF-biased superconducting point-contact quantum devices and a note on the properties of perfectly clean metal contacts. *J. Appl. Phys.* **41**, 1572–1580, 1970.

CSC – Scientific Computing Ltd. | P.O.Box 405 | FIN–02101 Espoo | Finland
CSC – Tieteellinen laskenta Oy | PL 405 | 02101 Espoo

ISSN 0787–7498
ISBN 952–9821–88–3
Picaset Oy 2003